Optimization of Process Variables in Extrusion-Spin Coating

by

Sangjun Han

Bachelor of Science in Naval Architecture and Ocean Engineering
Seoul National University, 1995

Submitted to the Department of Mechanical Engineering
in partial fulfillment of the requirements for the degree of

Master of Science in Mechanical Engineering

at the

MASSACHUSETTS INSTITUTE OF TECHNOLOGY

June 1997

© Massachusetts Institute of Technology 1997. All rights reserved.

Author . . . .
Department of Mechanical Engineering
May 9, 1997

Certified by . . . .
Jung-Hoon Chun
Edgerton Associate Professor of Mechanical Engineering
Thesis Supervisor

Accepted by . . . .
Ain A. Sonin
Chairman, Departmental Committee on Graduate Students

Optimization of Process Variables in Extrusion-Spin Coating

by

Sangjun Han

Submitted to the Department of Mechanical Engineering
on May 9, 1997, in partial fulfillment of the
requirements for the degree of
Master of Science in Mechanical Engineering

Abstract

Several thousand independent processes are required to produce a single semicondoctor chip. This thesis focuses on one: the process of coating a silicon wafer with photoresist. The conventional spin coating method produces uniform photoresist coating of the desired thickness. However, conventional spin coating wastes 95% of the photoresist applied for every batch process. As photoresist is not recyclable, spin coating method is very inefficient. Moreover, an imminent increase in cost of photoresist has raised the demand for new coating technologies.

Various methods for improving coating efficiency have been investigated. Based upon a comprehensive literature search and theoretical analysis, dramatic increases in efficiency and reductions in costs proved to be possible with the optimization of the dispense stage in spin coating. In the novel dispense process developed in this thesis, extrusion-spin coating replaces the conventional dispense stage. A major advantage of this method is its compatability with current spin coating method: little modification of existing spin coaters is required for this new technology.

In this thesis, critical process variables for the process are presented and the effect of each upon the coating result is estimated. Theoretical analysis and experimental confirmation are conducted for each process variable. Each process variable is then optimized. Finally, using the optimized process variables, the design of the process for successful coating is illustrated.

Thesis Supervisor: Jung-Hoon Chun
Title: Edgerton Associate Professor of Mechanical Engineering

Acknowledgments

Two years that seemed everlasting have now become two seconds of memory. At this moment, nothing is left in my heart but gratitude for those who made the two seconds' memory worth each second.

My sincere and utmost gratitude goes to Prof. Chun who gave me the wonderful opportunity to work on this project and who was never hesistant to share his knowledge with his students.

I would like to thank my lab partner Jim who encouraged me every time I was in despair, taught me when I was astray, and showed me the right attitude not only toward research but also toward life. Thank you, Jim. I don't know what else to say.

I cannot rule out Hodos, my office mate who usually was an annoying 'TFA' but who also revealed–probably faked–his hidden kindness when others were in need. Thanks Hodos, you made my office life very delightful. In addition, I also thank Dr. Kaplan who I have never met but brought me the same quality of joy as Hodos.

I would like to thank all the other people in the heat transfer lab; Mike, Andy, Rick, Rudy, Hesham, Hyuksang, Matt, and Prof. Griffith for their friendliness throughout the whole time. I am going to miss all of those who are now ending their journey in MIT.

I would like to thank Fred Cote and Gerry Wentworth for teaching me everything I wanted to know about machining but was afraid to ask. You guys are truly the best!

I want to thank all my Korean friends. Thank you, Sokwoo Rhee for your excellent advice whenever I needed it. Thank you, Chun Kang for saving my life once. Thank you, Shinsuk Park for your rarely helpful advice. Thank you, Jungmok Bae for...I forgot what I am thanking you for. Thank you Kontong Pahng for setting a standard for MIT life. Thank you, Yookyung Baek for your delicious 'kimchi bokeumbob.' And thanks to all the others whom I have forgotten to mention.

I would like to thank Dr. Saka for his deep concern in our safety and for lending us his cleaning hood.

Contents

List of Figures

10

List of Tables

Nomenclature

h Wet thickness

h_{dry} Dry thickness

d Gap distance between extrusion head and substrate

l Length of the flow path in extrusion die

w Width of slit

s Length of slit

Q Flow rate

V_{sub} Coating speed (speed of substrate)

DR Draw down ratio $(\frac{d}{h})$

Ω Angular velocity

a_Ω Angular acceleration

μ Viscosity of fluid

ν Kinematic viscosity of fluid $(\frac{\mu}{\rho})$

ρ Density of fluid

g Gravitational acceleration

σ Surface tension of fluid

σ_{SV} Surface tension of the solid in equilibrium with the vapor

σ_{SL} Interfacial tension between solid and liquid

σ_{LV} Surface tension of the liquid in equilibrium with the vapor

Ca Capillary number $(\frac{\mu V}{\sigma})$

Re Reynolds number $(\frac{\rho V L}{\mu})$

Bo Bond number $(\frac{\rho g L^2}{\sigma})$

S_f Solids content in coating liquid (%)

L_{Ca} Capillary length

Be Beguin number $(\frac{\Delta P}{\rho g L_{Ca}})$

Le Lewis number $(\frac{Ca}{(h/L_{Ca})^{3/2}})$

R_f	Radius of fore meniscus
R_r	Radius of rear meniscus
θ_s	Static contact angle of the coating liquid
θ	Dynamic contact angle of the coating liquid
V_{upper}	Upper limit speed
V_{180}	The coating speed at which the dynamic contact angle reaches 180°
$V_{air\ entrainment}$	The coating speed at which air entrainment begins
e	Evaporation rate
h_R	Reference thickness
Ω_R	Reference angular velocity
$h_{spin\ off}$	Resulting thickness from spin off stage
h_0	Initial thickness
$V_{solvent}$	Volume of solvent
ρ_{sol}^0	Initial density of the solvent
μ_0	Initial viscosity of the solvent
$t_{spin\ off}$	Time for spin off stage
$t_{evaporation}$	Time for evaporation stage
t_{spiral}	Time for spiral coating
ε	Coating efficiency
$Vol_{dispesne}$	Total dispense volume

Chapter 1

Introduction

1.1 Background

Coating a wafer with photoresist is one of the processing steps required for producing a semiconductor chip. Currently, spin coating is the most widely accepted method in the semiconductor industry. However, conventional spin coating method is quite inefficient. As photoresist is not recyclable, the waste is a serious potential environmental problem. Moreover, due to the imminent price increase of the newer generation of photoresist, the conventional spin coating method will not be cost-effective. Therefore, more efficient coating technologies are in high demand.

1.2 Coating efficiency

Efficiency is defined as the percentage of photoresist remaining at the end of the coating process. Figure 1-1 illustrates the improvement in coating efficiency in the past [1, 8, 18]. Efficiency of 12.56% in 1996 has been achieved using an experimental coater.

Conventional spin coating method requires a minimum of 4 ml dispense to acquire complete coverage with the desired uniformity for a 200-mm wafer. When the uniform coating thickness is 1 μm, the efficiency is only 4%. Therefore, 96% of the applied photoresist is thrown away for every spin coating process. Figure 1-2 illustrates the

15
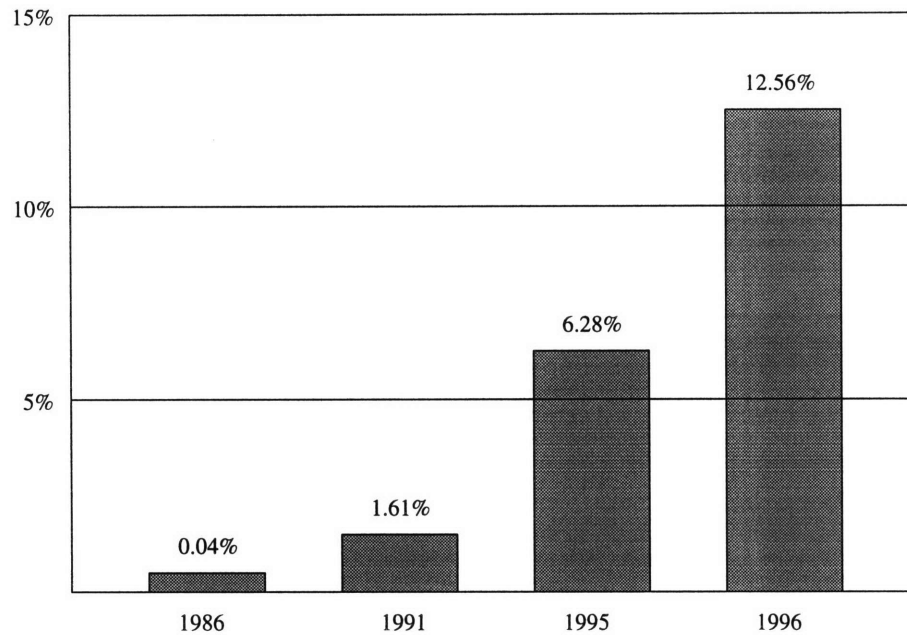
Figure 1-1: Historical improvement of coating efficiency. 25% solids content percentage was assumed for all coating liquids.

coating efficiency attainable with three different types of photoresist. Differences in coating efficiency result from the different solids content of each photoresist. Type A photoresist results in the highest coating efficiency among the three because it contains the least amount of solids content for the same volume.

1.3 Requirements for new coating technology

1.3.1 Coating efficiency

Improving coating efficiency is one of the major goals of the development of the new coating technology. Though efficiency of 12.56% was obtained in 1996 with 1 ml total dispense of photoresist, uniformity and defect levels were unacceptable for mass production. Thus, the initial goal of this research will be to achieve coating efficiency of 12.56% with acceptable uniformity and defect levels.

16
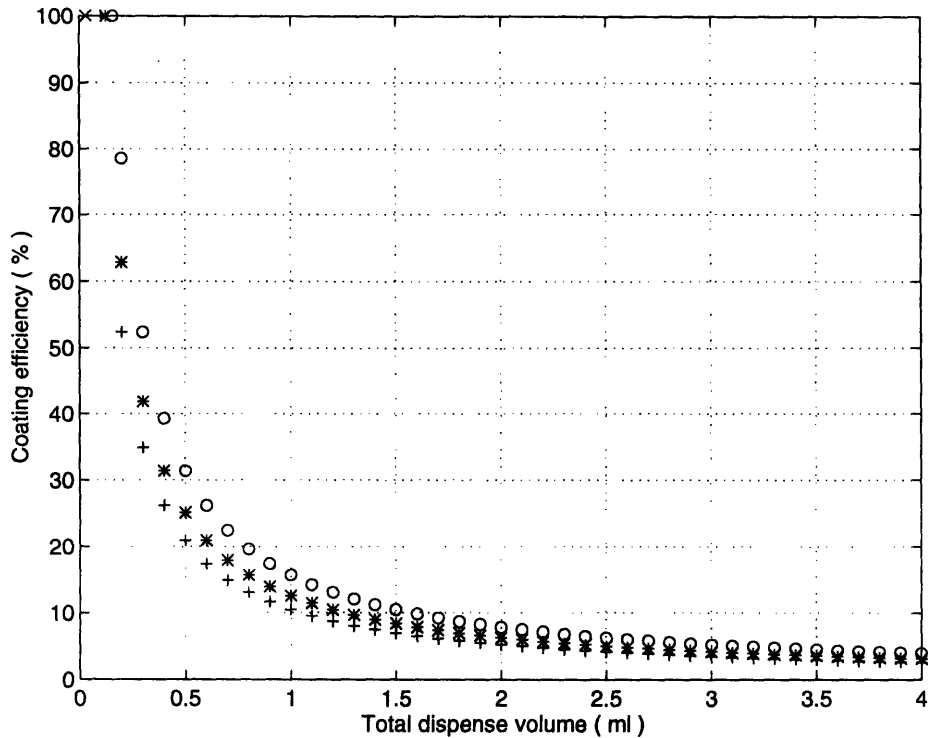
Figure 1-2: Coating efficiency attainable using three different types of photoresist. Type A: 20% solids content (o). Type B: 25% solids content (*). Type C: 30% solids content (+). Coating efficiency of 100% is achievable with dispense containing 3.1416e-2 *ml* of base material (x).

1.3.2 Coating uniformity and defect level

Coating uniformity across a wafer is represented by deviation from the mean thickness. As implanted patterns require increasingly more complex geometry in lithography, uniformity has to be improved correspondingly. In 1986, the required uniformity was ± 100 Å [25]; today, uniformity of ± 25 Å with 3σ is required.

Defects must be eliminated as far as possible for they can cause serious failure in the fabricated semiconductor chips. The defect level of the new coating technology should be at least that of the conventional spin coating method.

1.3.3 Coating time

Coating time is a very important parameter in the aspect of production rate. Conventional spin coating takes 30-45 seconds for the coating time. A new coating method should not exceed the current limit.

1.4 Development of new coating technology

Various methods for improving coating efficiency was investigated. Undergoing through numerous literature searches and theoretical analyses, it was concluded that optimizing the dispense stage can dramatically improve the efficiency. The core of "extrusion-spin coating" is replacing the conventional dispense stage with an extrusion method. An extrusion-slot coating method was adopted to optimize the dispense stage.

Extrusion coating and spin coating methods will be discussed in more detail. Extrusion-spin coating is evaluated by both theoretical analysis and experimental results. Finally, process variables of extrusion-spin coating are optimized to attain the best coating result.

Chapter 2

Extrusion-Spin Coating

2.1 Spin Coating

Spin coating is today's predominant method of applying thin layers of photoresist to wafers in the semiconductor industry. Spin coating is well adapted to the fabrication of integrated circuits, in which a uniform, adherent, defect-free polymeric film of a desired thickness has to be produced over an entire wafer. Many factors contribute to its popularity but most of all, consistency and simplicity of the application are the major attractions. Figure 2-1 shows how photoresist is applied on the wafer through a nozzle. After the dispense, the wafer is spun at high angular velocity to acquire the desired film thickness. The current target thickness in industry is 1 μm $\pm$ 25 Å. the following sections discuss in detail the conventional spin coating method, theoretical modeling, and the area to be improved.

2.1.1 Operation of spin coating batch process

The basic operation of spin coating consists of three stages as illustrated in Figure 2-2: deposition; spin-up; and spin-off. In the deposition stage, the coating liquid is applied on the wafer through a nozzle. A portion of the applied liquid immediately wets the substrate, displacing the air and gas that has been covering the substrate. In the spin-up stage, the wafer starts spinning at an acceleration of a_Ω. Consequently, centrifugal

19
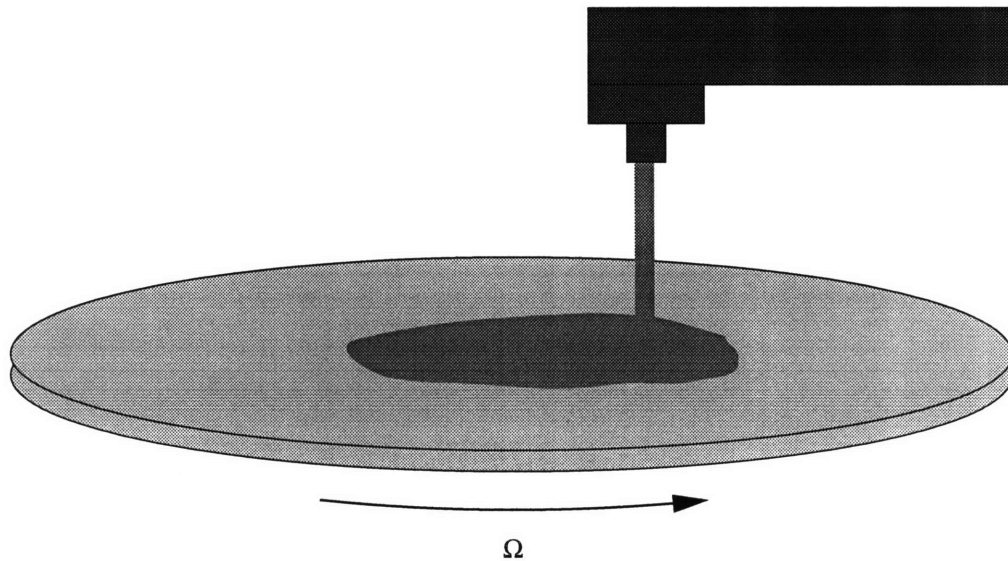
Figure 2-1: Spin coating method.

force causes the liquid to spread out and wet the entire substrate. In the spin-off stage, excess liquid is removed from the substrate. The liquid flows radially under centrifugal force and flies off the spinning wafer breaking into many droplets. On the substrate, a film of nearly uniform thickness is left which attains better uniformity as it thins out further. The solvent evaporates throughout the whole process but mostly takes place in the spin-off stage as the thickness of the coated film becomes thinner and thinner as illustrated in Figure 2-2 (c).

2.1.2   Possible defects from spin coating

Although using a minimum amount of photoresist is desirable in the aspect of efficiency, the lower limit of the amount of the photoresist must be determined considering three different factors: complete coverage; uniformity; and defect levels. To attain a successful coating, complete coverage has to precede all other conditions. Uniformity and defect levels are closely interrelated. Once uniformity over the whole wafer is obtained, defects are not to be detected in coated layer. However, due to the nonlinear dynamics of spin coating process, as the volume of applied photoresist is

(a) Deposition

(b) Spin-up a_Ω

(c) Spin-off $\Omega 1$ $\Omega 1$
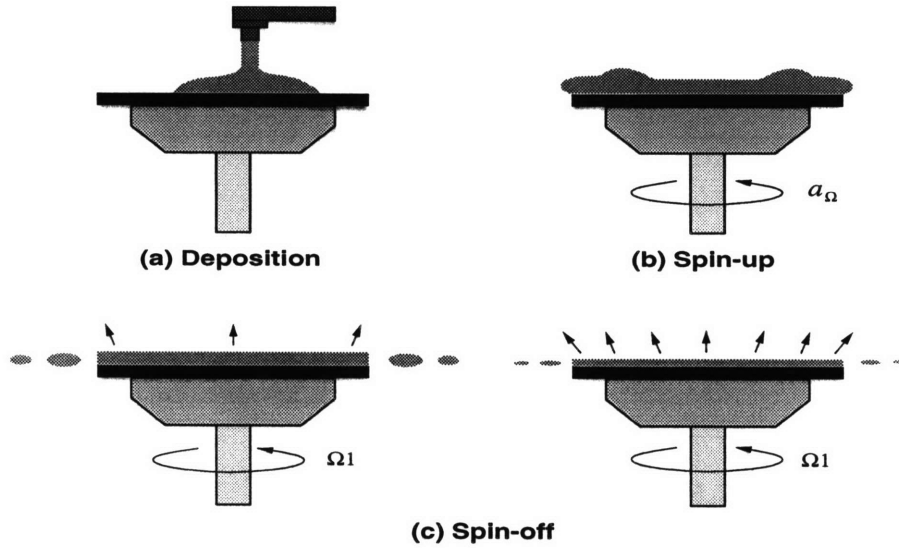
Figure 2-2: Stages of the spin coating batch process. The number of arrows in (c) represents the evaporation rate of the solvent.

reduced, various kinds of defects start to appear.

The most common defects in spin coating are voids, comets, and striations. Voids are the spots left uncoated after a coating cycle. The presence of voids implies that the amount of applied photoresist is not sufficient to coat the whole wafer. In such a case, adding more resist is the only solution to the problem.

Submicron particles encapsulated in the resist layer can cause nonuniformity as shown in Figure 2-3. These types of streaks with a particle nucleus are often called "comets." The region of comets are characterized by a thinner layer of coating. To eliminate "comets," particles must not be allowed in coating at any cost. Striations are strips that form toward the edge of a wafer due to molecular interactive attraction between photoresist particles. When the wafer is spun at high speed, due to the attraction, some streams of photoresist attracts others which causes the photoresist to spread unevenly as shown in Figure 2-4. As a consequence, the areas where striation takes place have thinner coating than other areas.

21
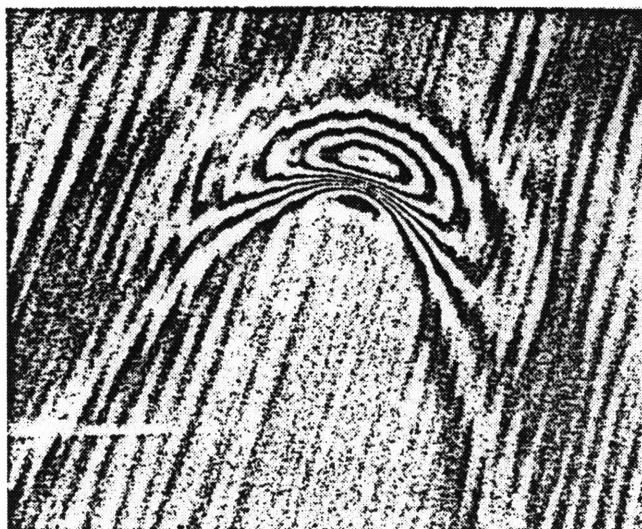
Figure 2-3: Particle-induced coating nonuniformity.
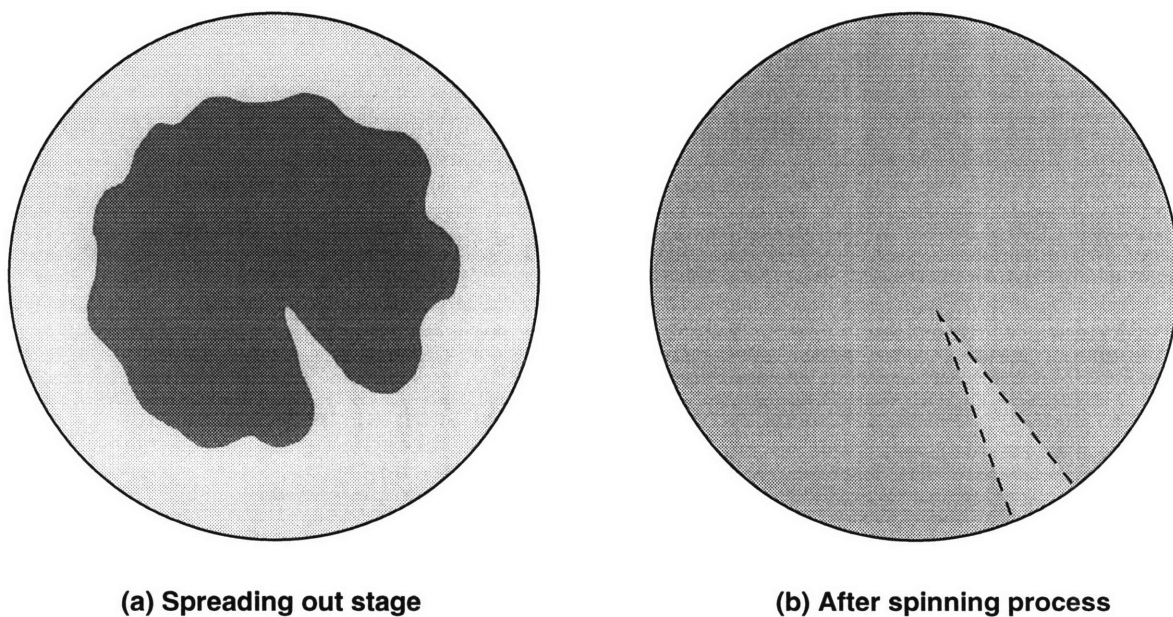
(a) Spreading out stage

(b) After spinning process

Figure 2-4: Striation of coated wafer. Uneven spreadout of resist in spin-on and spin-off stages causes striations represented by dotted line (- -) after spinning process.

2.1.3 Theoretical modeling of spin coating

Emslie *et al.* [11] have developed the model of liquid spreading over a spinning disk. At the outset, the following assumptions were made for simplicity:

1. The rotating disk is infinite in extent.

2. The plane is horizontal so that there is no radial gravitation components.

3. The liquid is not viscoelastic, i.e., the liquid is Newtonian.

4. The liquid layer is radially symmetric.

5. The liquid layer is so thin that differences in gravitational potential normal to the surface of the disk have negligible effect in distributing the liquid compared with the effect of centrifugal forces.

6. The liquid layer is so thin that shear resistance is appreciable only in horizontal planes.

7. The radial velocity is so small everywhere that Coriolis forces may be neglected.

In cylindrical coordinates (r, θ, z), the force balance between the viscous drag and centrifugal forces per unit volume will give:

$$-\mu\frac{\partial^2 v}{\partial z^2} = \rho\Omega^2 r \tag{2.1}$$

where μ is the fluid viscosity, ρ is the fluid density, Ω is the angular velocity of the wafer, and v is the linear velocity of the fluid toward the edge of the wafer.

Equation 2.1 can be integrated employing two boundary conditions: $v=0$ @ $z=0$ and $\partial v/\partial z=0$ @ $z=h$, resulting in:

$$v = \frac{1}{\mu}\left(-\frac{1}{2}\rho\Omega^2 r z^2 + \rho\Omega^2 r h z\right) \tag{2.2}$$

From Equation 2.2, the flow rate per unit length of circumference, q, can be obtained:

$$q = \int_0^h v\,dz = \frac{\rho\Omega^2 r h^3}{3\mu} \qquad (2.3)$$

From mass conservation, differential equation for h is obtained:

$$r\frac{\partial h}{\partial t} = -\frac{\partial(rq)}{\partial r} \qquad (2.4)$$

As the behavior of the film thickness is of prime interest, by substituting the values of h from Equation 2.3 to Equation 2.4:

$$\frac{\partial h}{\partial t} = -C\frac{1}{r}\frac{\partial}{\partial r}(r^2 h^3) \qquad (2.5)$$

can be derived, where $C = \rho\Omega^2/3\mu$.

Since our experiment is based on an initially uniform distribution of photoresist, h is independent of radial distance from the center r and dependent only upon time t. In such a case, Equation 2.5 can be simplified as:

$$\frac{dh}{dt} = -2Ch^3 \qquad (2.6)$$

and thus:

$$h = \frac{h_0}{(1 + 4Ch_0^2 t)^{\frac{1}{2}}} \qquad (2.7)$$

where the constant h_0 corresponds to the initial height of the film. From Equation 2.7, it can be deducted that if the initial distribution of the film is uniform everywhere it will remain uniform throughout the whole spinning process. Equation 2.7 also shows that the thickness of the fluid layer decreases by a factor of $1/\sqrt{2}$ in a time $\tau = \frac{1}{4Ch_0^2}$. Thus, a thicker coating tends to thin out at a faster rate than a thinner coating.

2.1.4 Development of dispense stage in spin coating

Spin coating has been successfully used to acquire uniform coating thicknesses. However, due to its low-efficiency, many attempts have been made to minimize the amount

Center Dispense   **Forward radial dispense**   **Reverse radial dispense**
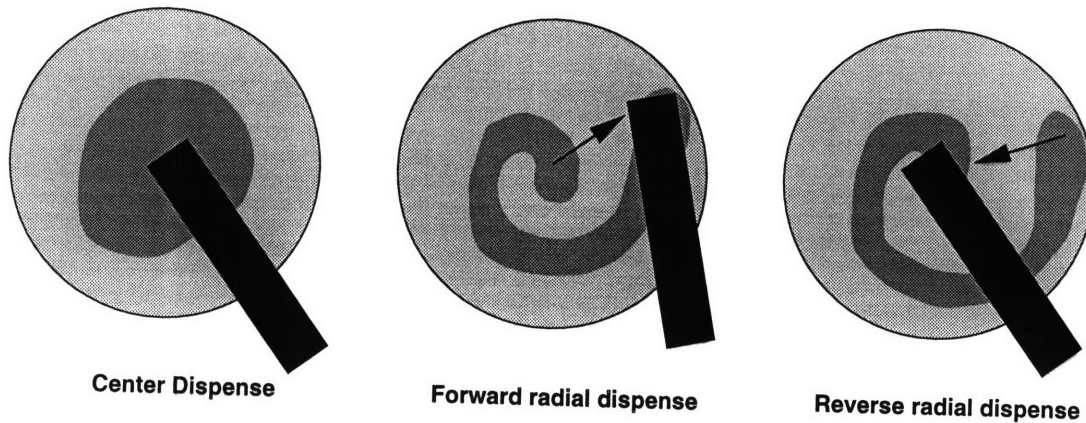
Figure 2-5: Different dispense methods for spin coating.

of coating liquid by optimizing each stage. The result was investigation of various dispense methods since other stages were not as flexible for modification as the dispense stage. Figure 2-5 shows three different dispensing methods: center dispense; forward radial dispense; and reverse radial dispense. Of those, the reverse radial dispense method is accepted experimentally as the one that provides the desired uniformity with the least amount of photoresist.

2.1.5 Further development of dispense stage

The purpose of testing various dispense methods in spin coating is to optimize the deposited pattern of photoresist. When the pattern is optimized in the deposition stage, it is easy to acquire a fully-covered and uniform initial coating at the beginning of the spin-off stage. However, deposited patterns have been investigated mainly by experiments since it is almost impossible to analyze theoretically the behavior of such patterns as shown in Figure 2-5 (b) and (c).

It was concluded that only the completely new dispense method, which is also theoretically analytical, can minimize the waste while maintaining a uniform initial thickness. The extrusion coating method has been chosen for the application. It is discussed in detail in the following sections.
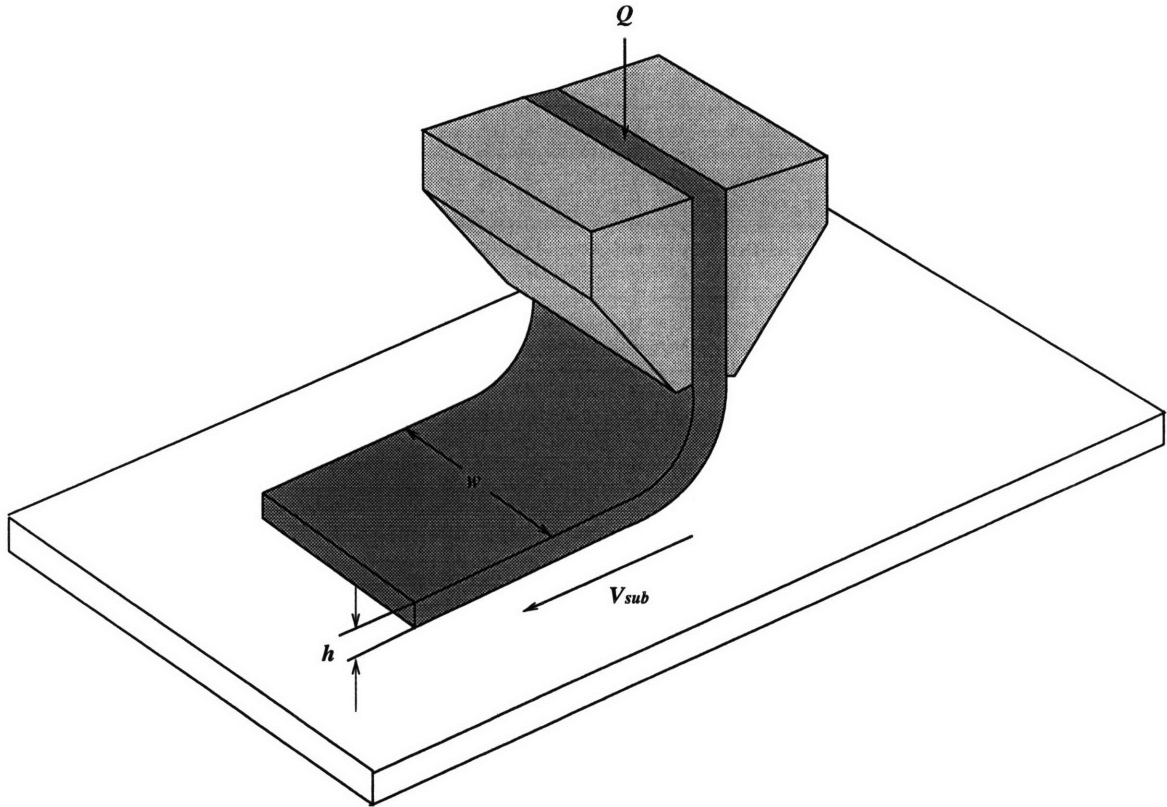
Figure 2-6: Extrusion coating.

2.2 Extrusion coating

2.2.1 Terminology

A coating flow is a fluid flow that is used to cover a surface area with a thin layer. Once the coating film is laid upon the surface, evaporation takes place leaving the solid contents of the coating liquid. The "premetered" coating represents the method by which the coating thickness can be controlled by other parameters such as coating speed, coating width, and flow rate. When all fluid fed to the extrusion die is coated as shown in Figure 2-6, the wet thickness, h, can be expressed as:

$$h = \frac{Q}{V_{sub}w} \qquad (2.8)$$

where Q is the flow rate, V_{sub} is the coating speed, and w is the width of the slit in the extrusion head, respectively.

At the end of a complete coating cycle, all solvent in the coating liquid is evapo-
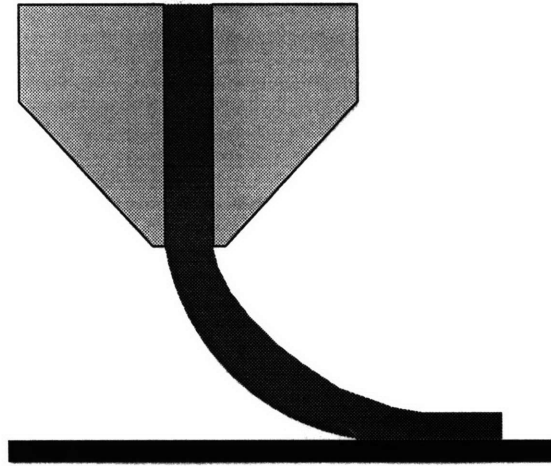
Figure 2-7: Curtain coating.

rated to leave only the solid content. The final dry coating thickness, h_{dry}, is expressed in terms of solids content and wet coating thickness:

$$h_{dry} = \frac{S_f h}{100} \tag{2.9}$$

where S_f is the solids content. Solids content specifies the percentage of the photoresist that will remain as a solid after all the solvent has been evaporated. It is expressed as the percentage of the original liquid mass left behind as a dried mass.

The term "extrusion coating" is used differently in various applications. In this thesis, "extrusion coating" will be used comprehensively for all coating techniques in which fluid is squeezed from an extrusion die through narrow slits.

The extrusion coating method can be subdivided into two major categories: curtain coating and extrusion-slot coating. In curtain coating, a flow is squeezed from an extrusion head to be laid upon a substrate as illustrated in Figure 2-7. The name curtain coating comes from the way the extruded flow draws down like a curtain.

Extrusion-slot coating is sometimes called bead coating for its major characteristics is the bead formed on the fore coating lip as illustrated in Figure 2-8. The gap distance between the extrusion die and substrate has to be small enough for a bead to be formed on the fore lip.

Extrusion-slot coating is conducted when unformity and the level of defects are

27
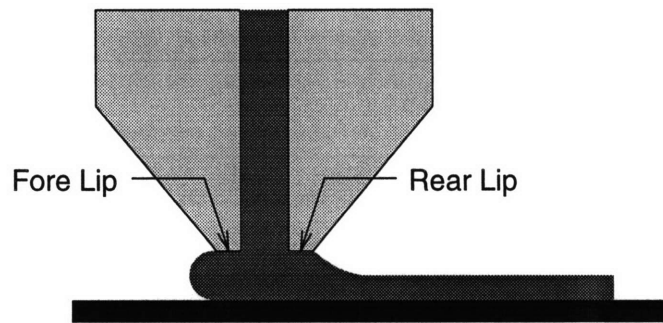
Figure 2-8: Extrusion-slot coating.
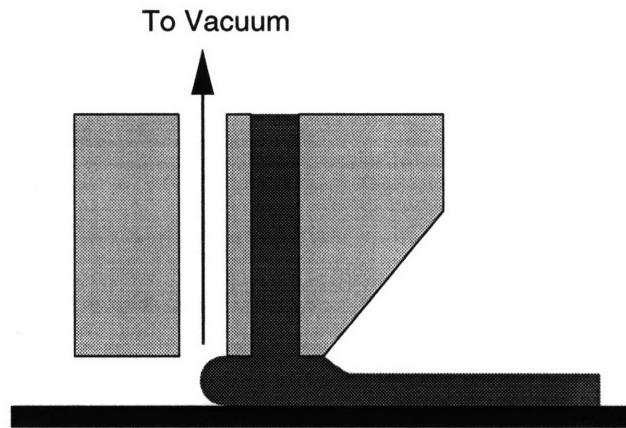
Figure 2-9: Extrusion-slot coating with vacuum.

considered to be the critical parameters. It has been shown in many theoretical analyses and experiments that in order to create such defect-free, smooth coatings, the well-shaped bead must be formed and maintained on the fore lip and throughout the coating process. Vacuum can be introduced to create an adequate pressure difference across the bead to help maintaining a well-shaped bead [22]. Figure 2-9 shows the extrusion-slot coating with a vacuum introduced at the fore coating lip.

(a) Air entrained

(b) Swelling and weeping at fore meniscus

(c) Ribbing

(d) Rivulets

(e) Chatter
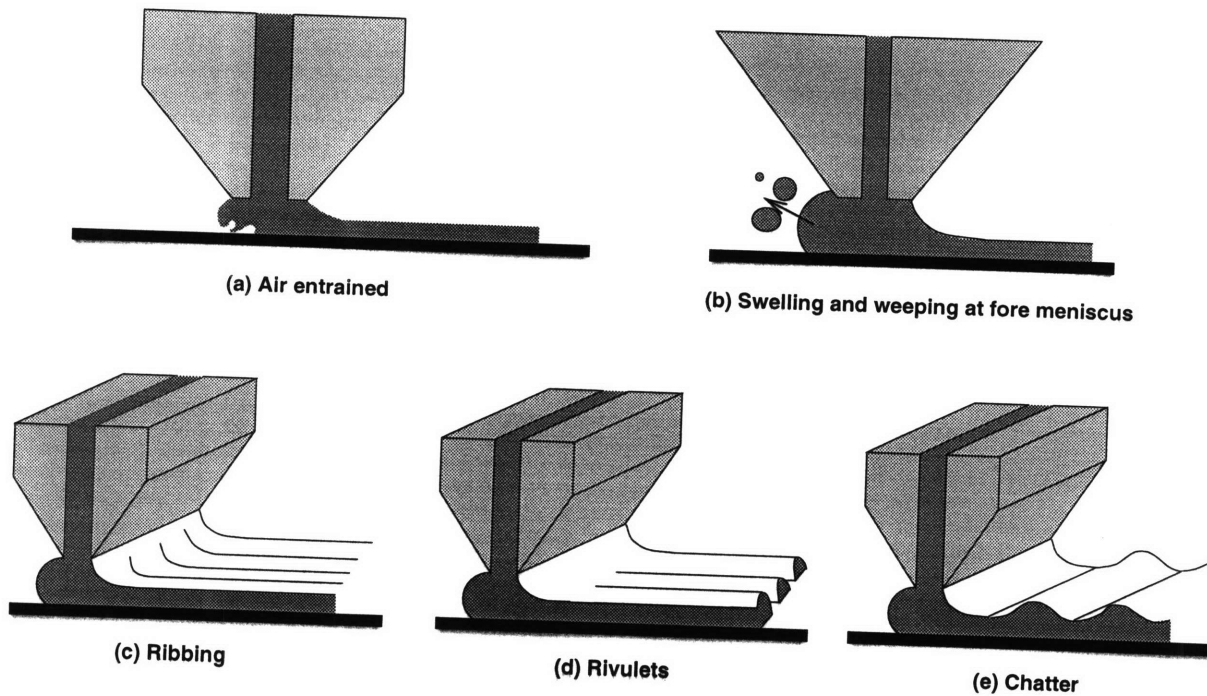
Figure 2-10: Various possible defects from extrusion-slot coating.

2.2.2 Possible defects from extrusion-slot coating

Figure 2-10 shows the most common defects resulting from extrusion-slot coating. Defects from extrusion-slot coating are mainly caused by coating speed. The upper speed limit is the speed below which uniform coating is made with no defects. Defects that can be caused by excessive coating speed are air entrainment, ribbings, and rivulets. When coating speed exceeds the upper limit, the coating liquid extruded from the fore lip becomes unstable and allows the air to be entrained in the bead as illustrated in Figure 2-10 (a). This unstable phenomenon also occur in the rear lip, causing ribbings as in Figure 2-10 (c). If the coating speed surpasses the limit even further, rivulets are formed as in Figure 2-10 (d), leaving the part of substrate uncoated. Figure 2-10 (e) shows chatter which is the fluctuating phenomenon of coating liquid. Chatter, ribbing, and rivulets are also related to the surface tension of the coating liquid. Swelling and weeping at fore meniscus, as in Figure 2-10 (b), appear when the vacuum rate is too high.

Since defects are mostly caused by excessive coating speed, an upper speed limit for a successful coating has to be determined.

29
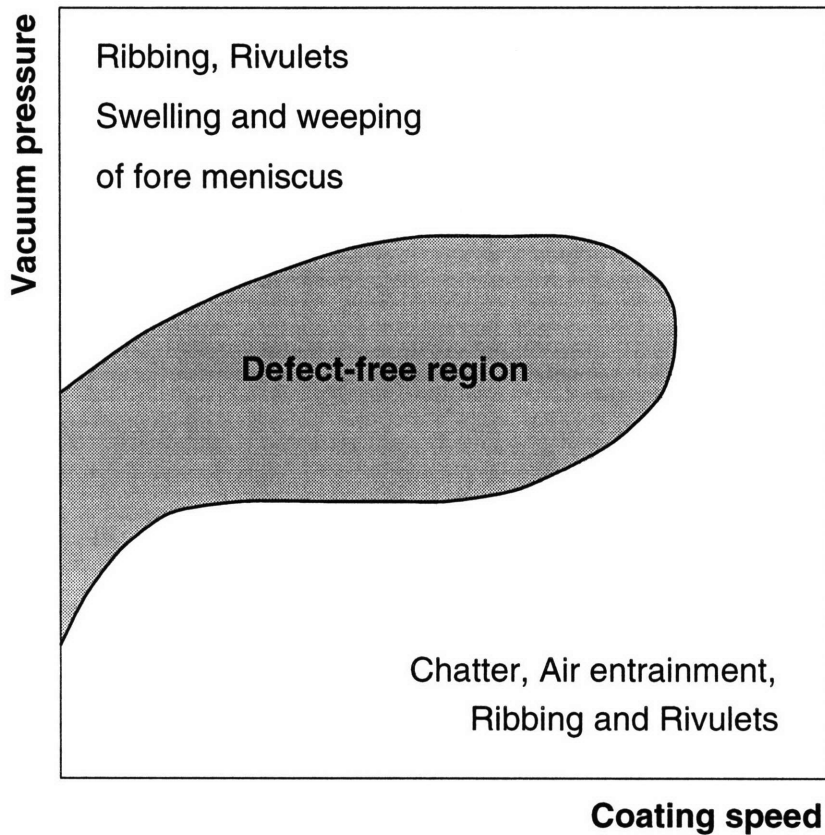
Figure 2-11: The schematic window of coatability for extrusion-slot coating. Note that ribbing and rivulets can occur at both high coating speed and high vacuum pressure.

2.2.3   The window of coatability

Lower and upper coating speed limits are influenced by many factors. Usually, a low coating speed is not desirable for productivity and high coating speed is constrained by problems such as incomplete coverage, nonuniformity, and defects.

In the parameter space of coating speed, vacuum pressure, film thickness, and other process variables, a region exists within which the coated film is free of unacceptable defects: this region is called the "window of coatability."

The window of coatability can be acquired from experimental data. Lower limits and upper limits of coating speed and vacuum rate are to be established by various constraints such as coating efficiency, unformity, defect level, etc. Sartor [22] has established a window of coatability for extrusion-slot coating for many different gap
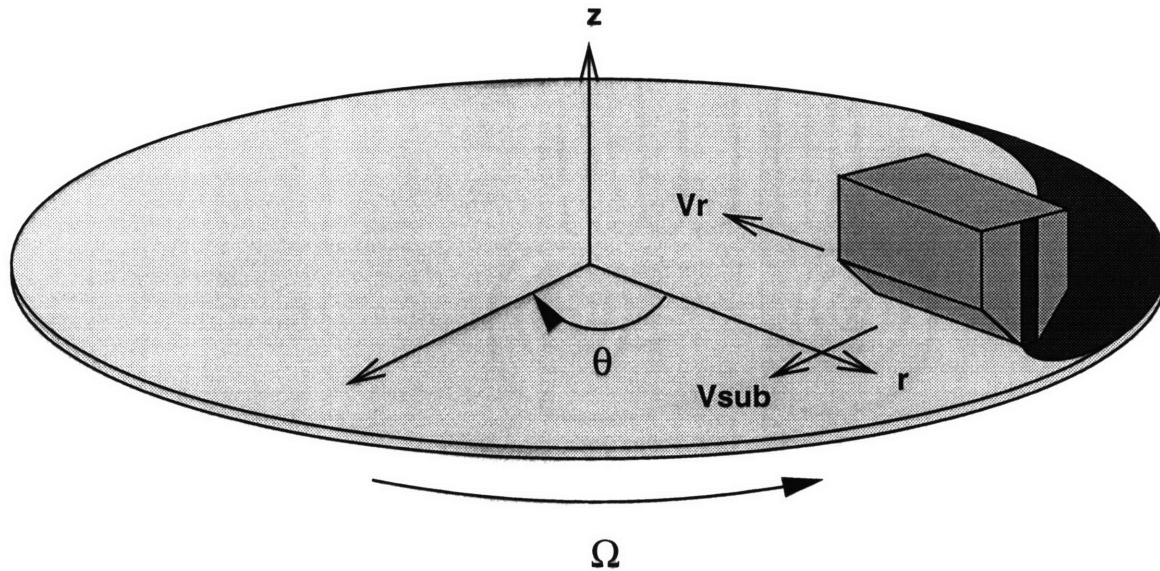
Figure 2-12: Illustration of extrusion-slot coating process.

distances. The schematic operating window for two-dimensional, steady, defect-free coating is illustrated in Figure 2-11. Chatter, air entrainment, ribbing, and rivulets appear in the region where either vacuum pressure is too low or coating speed is too high. Ribbing and rivulets can also occur when vacuum pressure is too high. Swelling and weeping of fore meniscus are defects that appear only in high vacuum regime. Chapter 4 contains a detailed explanation of these defects.

2.3 Description of extrusion-spin coating method

The extrusion-spin coating method replaces the dispense stage of conventional spin coating with an extrusion-slot coating method. As most of the waste in spin coating is created in the spin-off stage, replacing this stage with extrusion-slot coating will improve efficiency tremendously. Figure 2-12 is a schematic diagram of the extrusion-slot coating process.

(a) Squre sweep coating   **(b) Discrete radial coating**
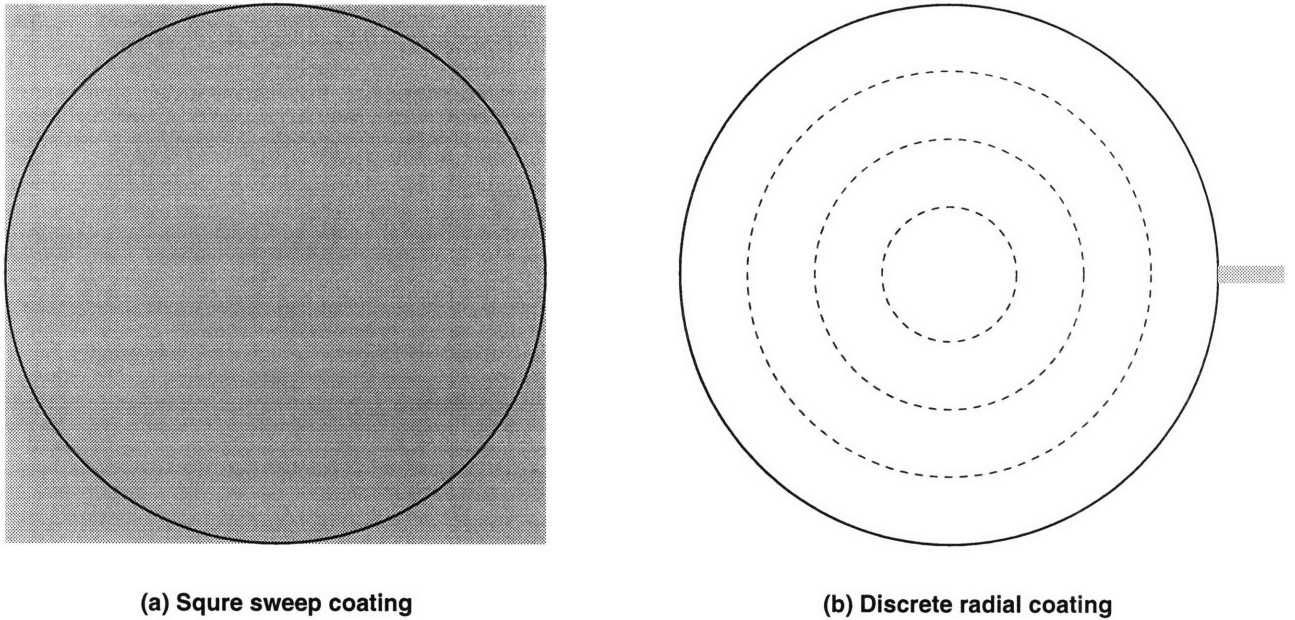
Figure 2-13: Different applicable coating patterns for extrusion-slot coating.

2.3.1 Various coating patterns

Various coating patterns are applicable to extrusion-slot coating. Figure 2-13 shows two possible patterns. Squre sweep coating can be conducted by using an extrusion head whose width is of the same length or slightly longer than the diameter of the wafer. The entire wafer is coated in one path as the extrusion head sweeps over it.

Discrete radial coating is characterized by the position of the extrusion head in each coating process. The extrusion head is placed in one radial position. The wafer is rotated a turn, leaving a stream of coated layer. Then the extrusion head is moved to the next radial position, making another stream of coated layer. It repeats the pattern until the entire wafer has been coated.

However, two principle goals must be satisfied in choosing a coating pattern: high efficiency and continous coating. High efficiency is the ultimate goal of this new method. Continuous coating is essential in extrusion-slot coating to maintain a well-shaped bead as was mentioned in Section 2.2.1. Square sweep coating is effective in maintaining a well-shaped bead but its coating efficiency is relatively low, as illustrated in Figure 2-14. Discrete radial coating demonstrates high coating efficiency
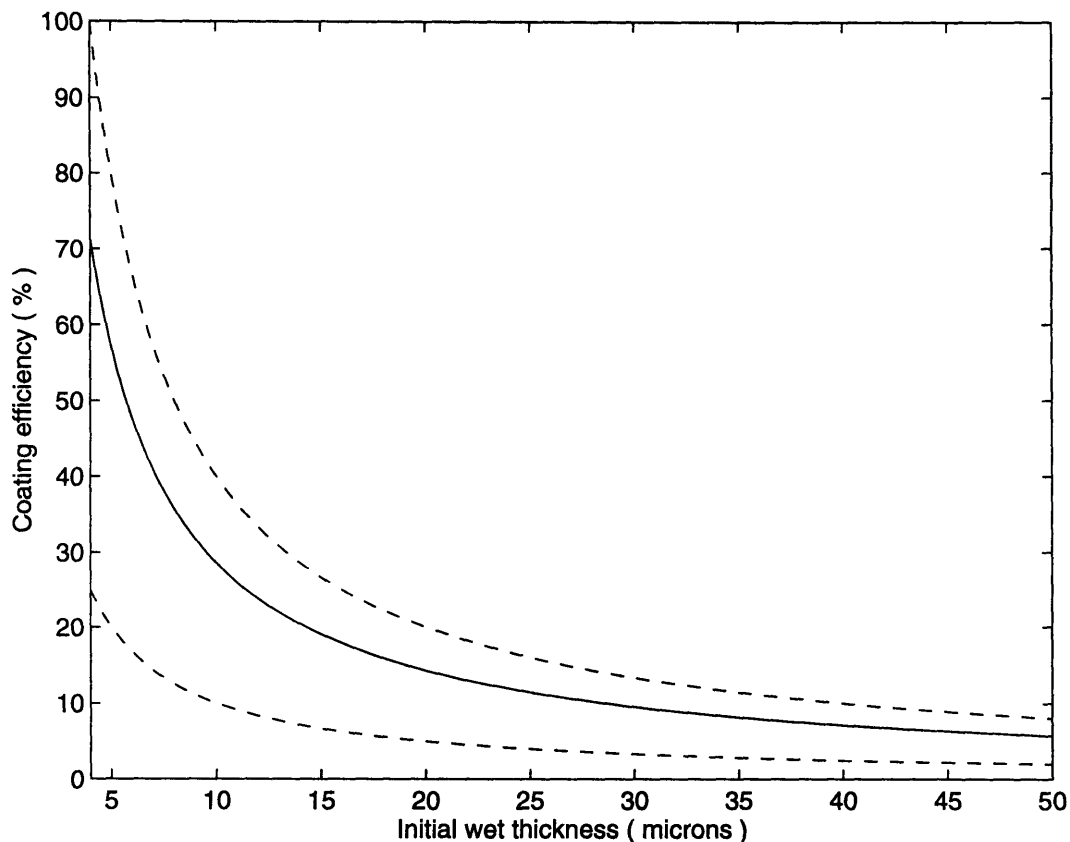
Figure 2-14: Efficiency comparison among square sweep coating, discrete radial coating, and spiral coating patterns. 25% of solids content was assumed for the coating liquid. Dotted line on top represent the coating efficiency using discrete radial coating. Dotted line on bottom represent the coating efficiency using squre sweep coating. Continuous line represent the coating efficiency using sprial coating pattern.

but the coating cannot be continuous since the extrusion head has to move to the next radial position after each rotation.

It was concluded that combining the merits of each method would result in the best combination, and thus, the spiral coating pattern has been adopted.

2.3.2 Spiral coating pattern

The spiral coating pattern (Figure 2-15) has been developed to have continuous extrusion-slot coating with high coating efficiency. The extrusion head moves toward the center while the wafer rotates at a changing angular velocity due to the varying location of extrusion head in r direction. Appendix A shows an analysis of the spiral motion.

33
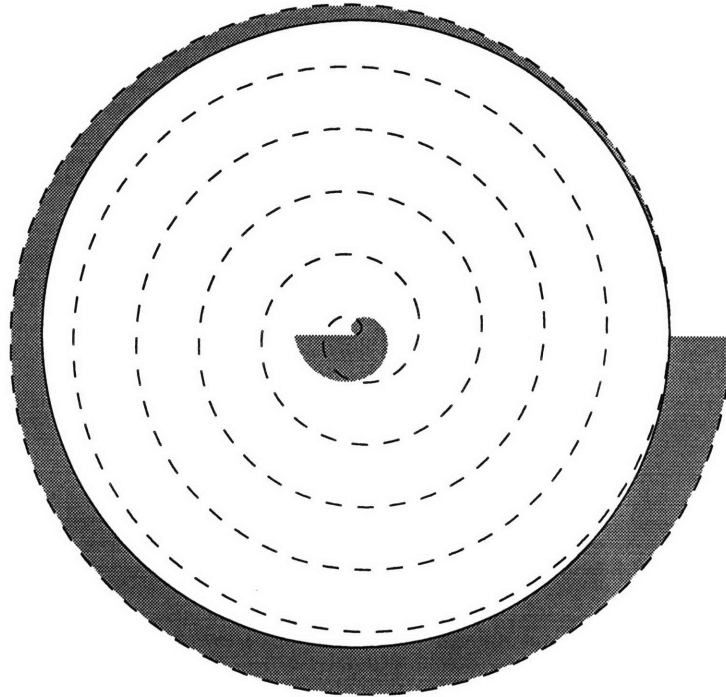
Figure 2-15: Spiral coating pattern formed on 200-mm wafer with extrusion head of 2 cm width.

The shaded region outside the circle in Figure 2-15 shows the initial dispense. Initial dispense is essential in extrusion-spin coating for two reasons. Photoresist at the tip of extrusion head usually dries out between two consecutive coating processes. Dry photoresist must not be dispensed on the wafer for it could cause nonuniformities. The second and more important reason is that extrusion-spin coating needs a stable coating bead. The coating bead is formed within the first rotation of the wafer.

The first rotation is also important for uniformity. At a certain point, capillary force exceeds gravitational force and all extruded flow piles on the edge of the wafer as illustrated in Figure 2-16. As a result, a thicker coating always forms on the edge of the wafer.

The shaded region at center of the wafer denotes the overlapped region. The overlap at the center is inevitable because the only way to avoid the overlap is to have infinite angular velocity at $r = 0$, which is physically impossible. Great care must be exercised to minimize the overlap to avoid any nonuniformities. Solutions to the center overlap problem are discussed in Chapter 6.

(a) Initial position   **(b) Contact position**   **(c) Dominant capillary force**
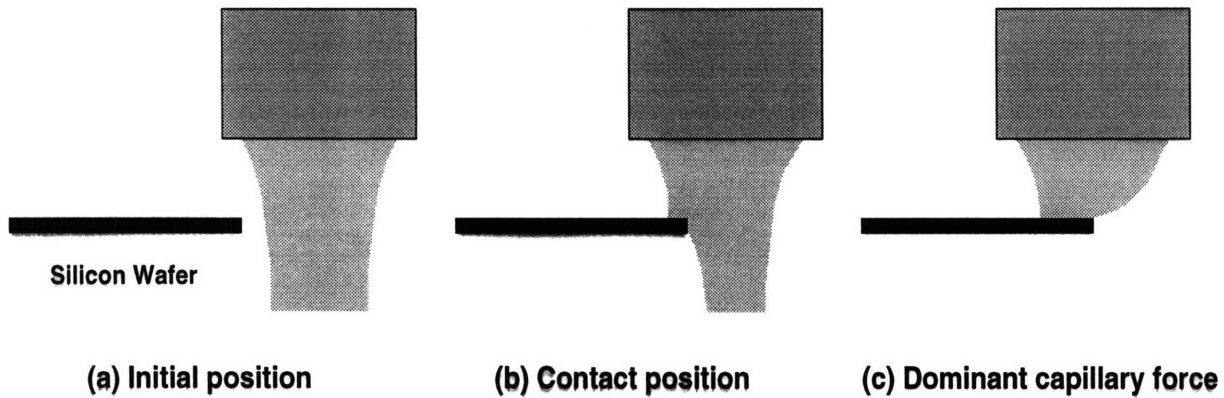
Figure 2-16: Bead formation at the edge of the wafer.

2.4   Advantages of extrusion-spin coating

Extrusion-spin coating surpasses conventional spin coating in two major aspects. Coating efficiency should be higher. Spin coating requires an abundant dispense of photoresist to assure that the initial thin layer covers the whole wafer. The initial uniform layer is obtained in the middle of spin-off stage at which most of the applied photoresist has been already thrown out. Extrusion-spin coating starts with that thin layer of coating, eliminating the waste. Thus it produces the minimum amount of waste, resulting in increased coating efficiency. Another advantage is the improved coating uniformity. To achieve an initial thin uniform layer with spin coating, an excessive amount of resist is required although nothing guarantees uniformity. On the other hand, with extrusion-spin coating, initial uniform thickness is assured since thickness is controlled by premetering. Emslie *et al.* [11] predicts that uniform coating on the wafer will remain throughout the spin coating process. Thus extrusion-spin coating will result in higher efficiency with better uniformity as compared to regular spin coating method.

Chapter 3

Design of Extrusion-Spin Coater

3.1 Overall description of the apparatus

A prototype extrusion-spin coater was built to conduct experiments with the extrusion-spin coating technique. Figure 3-1 illustrates the apparatus. An extrusion-spin coater consists of two major modules: an extrusion module and a spin coating module. The extrusion module comprises an X-Z motion table, optical sensor, extrusion head, and dispensing pump. The spin coating module refers to a spin coater whose major components are a vacuum chuck, spindle rod, and motor.

3.2 Design goals

In designing an extrusion-spin coater, three design goals were established: compatibility, flexiblity, and accuracy. The prototype was based on an existing spin coater, which ensures the compatibility with existing spin coaters. The extrusion head mount is designed to flexibly mount different types of heads. Accuracy was the highest priority when designing the prototype. Extrusion-slot coating must be conducted with precisely controlled position and coating speed. Components of the extrusion-spin coater were selected, focusing on the accuracy requirements.
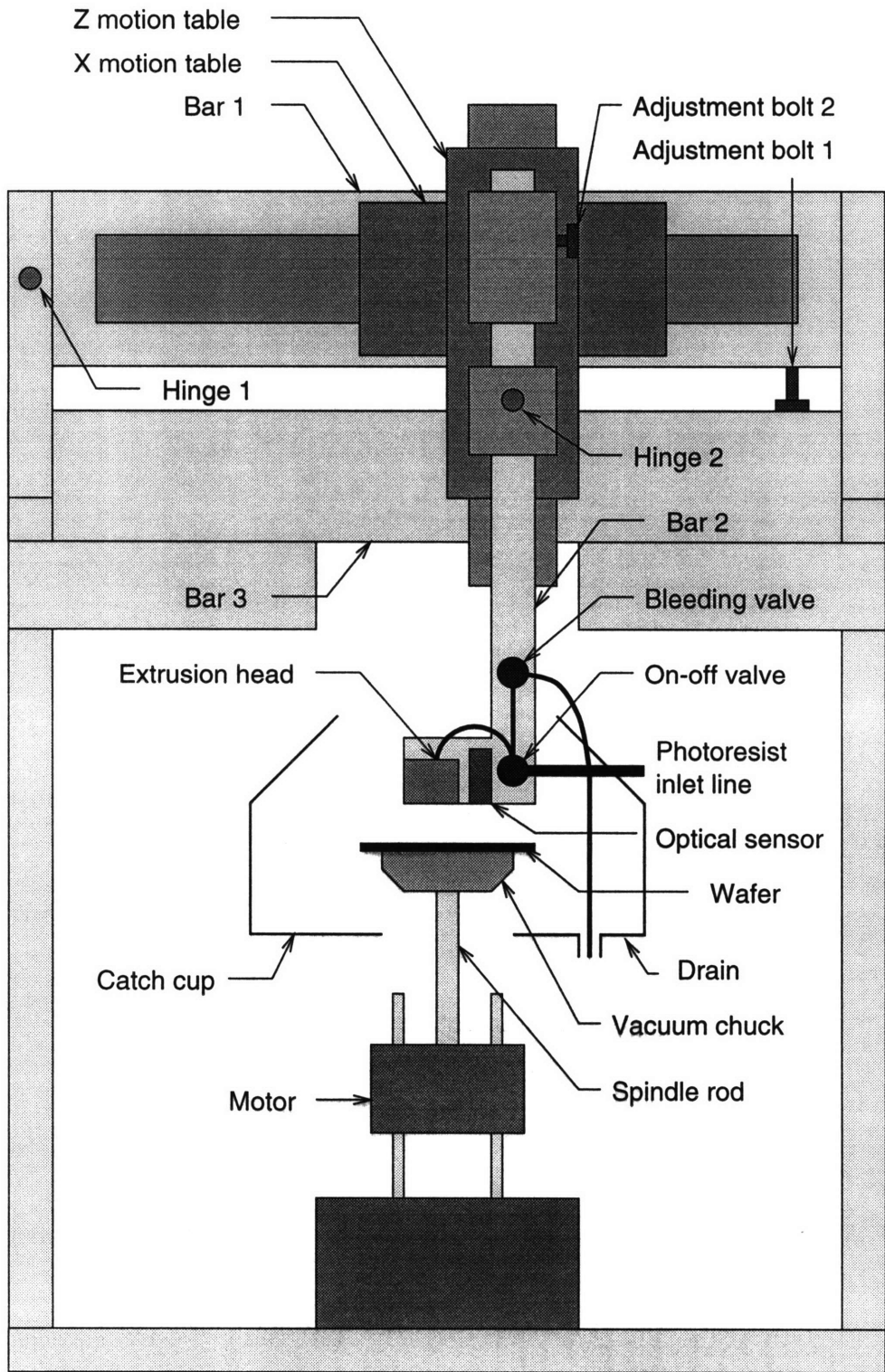
Figure 3-1: Perspective of extrusion-spin coater.
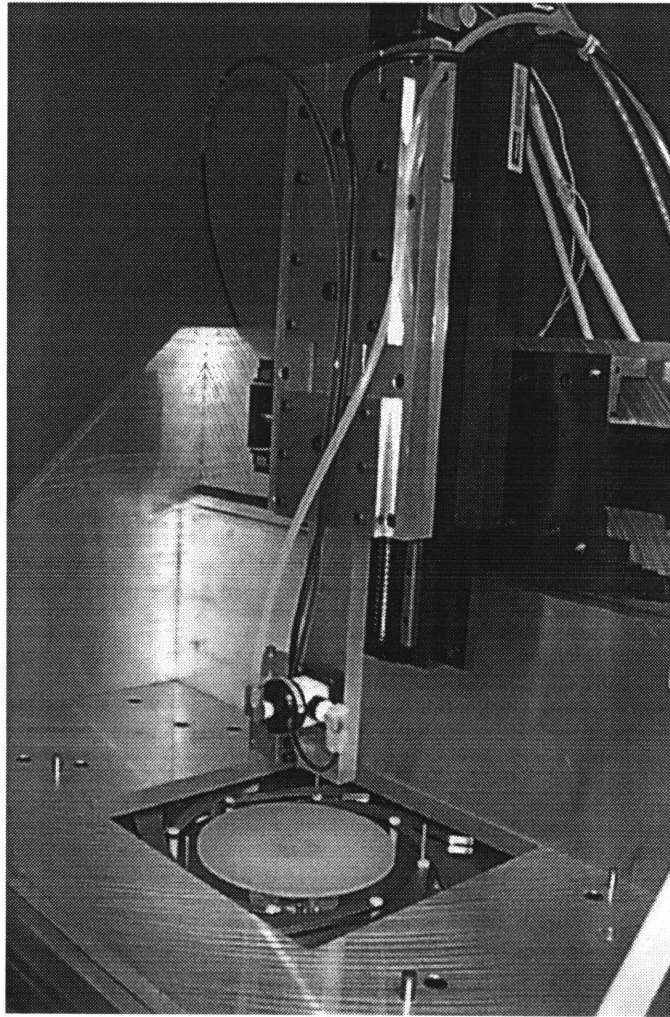
Figure 3-2: X-Z motion table.

3.3   Extrusion module

3.3.1   X-Z motion table

The X-Z motion table positions the extrusion head precisely for coating. A Daedal 800000 series table, shown in Figure 3-2, was selected to meet the requirement in terms of accuracy. Three accuracies were determined to be critical in our application: positional accuracy; straight line accuracy; and repeatability. Positional accuracy represents the precision level of table, which is 150 $\mu m/m$. Straight line accuracy is the deviation from the straight line when Z table is moving along X table. Straight line accuracy is 80 $\mu m/m$. Repeatability shows how accurately the same position can be reached. With tolerance of ± 5 μm, repeatability is satisfactory.

3.3.2 Optical sensor

A reflectance compensated sensor from Philtec was choosen for our application. The sensor measures the gap distance between the extrusion head and the substrate. The output voltage is only proportional to the distance between the sensor tip and the target surface. It is used for vibratory motion and applications in which the target rotates or translates in a direction perpendicular to the axis of the sensor. The sensor RC140L has sensitivity of 4.9065 $\mu m/mV$ and linear range between 5.51 and 6.17 mm with corresponding voltage changing from 1 to 3 volts with a tolerance of $\pm 0.5\%$.

3.3.3 Extrusion head

Gutoff [13] summarizes several designs of die internals in his paper. Figure 3-3 illustrates a typical T-die design. The extrusion head is composed of two separable extrusion die pieces and a shim. A shim of thickness s is inserted between the two pieces and then three are bolted tightly together to prevent leaks to any sides other than the aperture in the bottom. Photoresist is extruded through the aperture and is applied upon the slowly-spinning wafer. Due to the adhesiveness of the two materials, the thin film of coating is formed. The gap distance between extrusion head and the substrate has to be within the allowable range to prevent neck-ins (Figure B-1 in Appendix B).

3.3.4 Dispensing pump

A dispensing pump controls the flow rate of the extruded flow. A Gen-2^{Plus} photochemical dispense system from Millipore was selected for the application. It is a displacement pump with 0.08 ml/sec minimum flow rate and 0.01 ml/sec step volume. 70 kPa and 414 kPa clean air or nitrogen are required for the operation. A bleeding valve was installed later to decrease the minimum flow rate. As a consequence, the minimum flow rate was reduced to 0.035 ml/sec for AZ1512 and 0.011 ml/sec for AZ Deep UV resist (See Appendix C for pump calibrations).

(a) Shim   (b) Front view   (c) Side view

(d) Bottom view
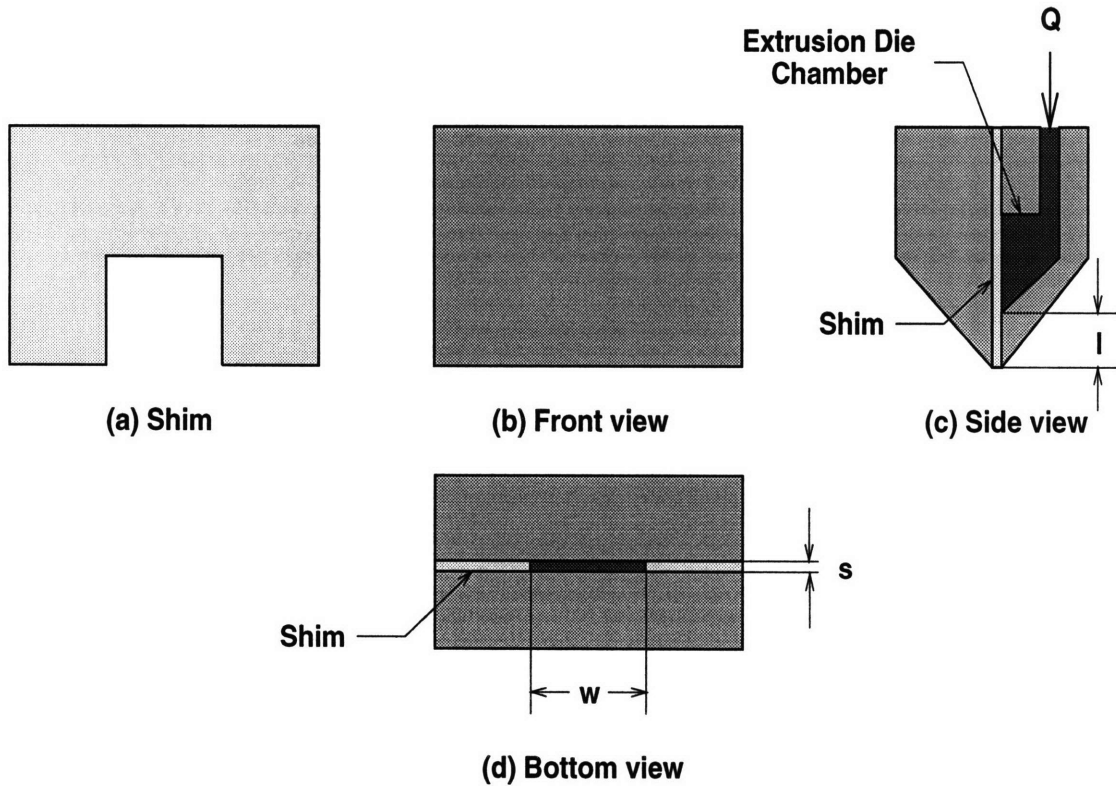
Figure 3-3: Extrusion head perspective.

3.3.5 Alignment issues

The biggest issue in designing an extrusion module was the alignment. Two alignments are critical in conducting experiments correctly: X motion table and the extrusion head. Both have to be perfectly aligned with the wafer. Three adjustment bolts were used to execute the neccessary alignments. Adjustment bolt1, as indicated in Figure 3-1, aligns the X motion table with the wafer by rotating bar1 with respect to hinge1. Adjustment bolt2 aligns the extrusion head with the wafer coarsely by rotating bar2 with respect to hinge2. There is another adjustment bolt3 behind bar3 that is not shown in Figure 3-1. Its basic function is to fine-tune the alignment of the X motion table with the wafer.

3.4 Operation of extrusion module

One cycle of the extrusion coating process consists of four major stages as illustrated in Figure 3-4. In the first stage, the extrusion head scans over surface of the wafer, recording the gap distance between the wafer and extrusion head using the sensor. In the next stage, the extrusion head comes down to the z position at which the head will be away from the wafer by the required gap distance. In the third stage, the wafer is coated. The extrusion head moves toward the center of the wafer dispensing photoresist while it gets feedback from the sensor to keep the gap distance constant. At this stage, the wafer keeps rotating with a changing angular velocity profile to keep the linear speed of the extrusion coating constant. A spiral pattern as indicated in Figure 2-15, is formed as velocity toward the center varies along the radial position and tangential velocity is kept constant. In the last stage, the extrusion head is pulled away from the wafer after dispensing the proper amount of photoresist on center region.

3.5 Spin coating module

The spin coating module is from an SVG 90SE track system. Basic components for the spin coater are a vacuum chuck, spindle rod, and motor. A vacuum chuck, as its name implies, uses 77 kPa vacuum to hold a wafer. A spindle rod connects the chuck and the motor, transmitting torque generated from the motor. The rod mechanism is critical in our experiments for its dynamics is directly related to the spinning motion of the wafer. In order to keep the wafer absolutely flat during the coating, the spindle rod cannot have any unpredictable dynamics. The Pacific Scientific motor is controlled by SC755 controller from Pacific Scientific Inc.

The spin coating process is required to attain a desired coating thickness and uniformity. The final coating thickness can be controlled by varing the spin speed. Conventionally, a spin speed between 3000~5000 rpm is used to attain 1 μm thickness.

41
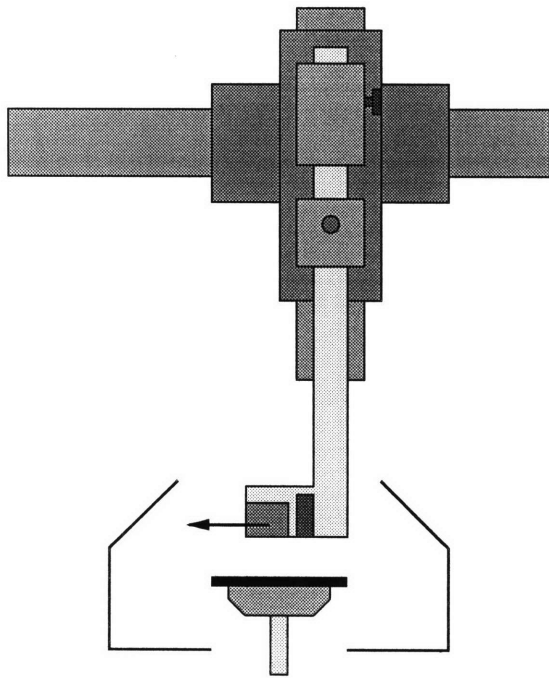
(a) Scanning the surface
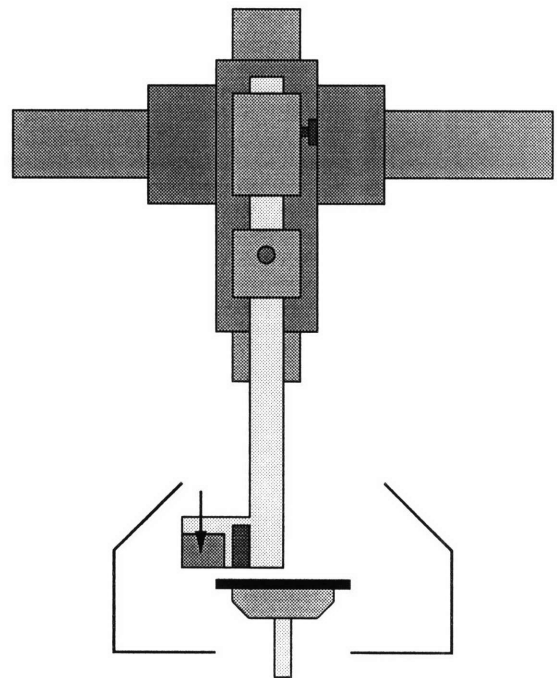
(b) Locating the coating outset position
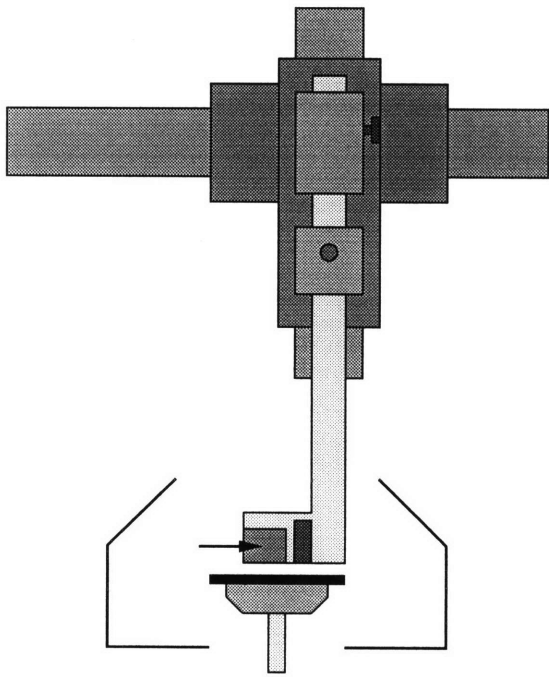
(c) Coating wafer
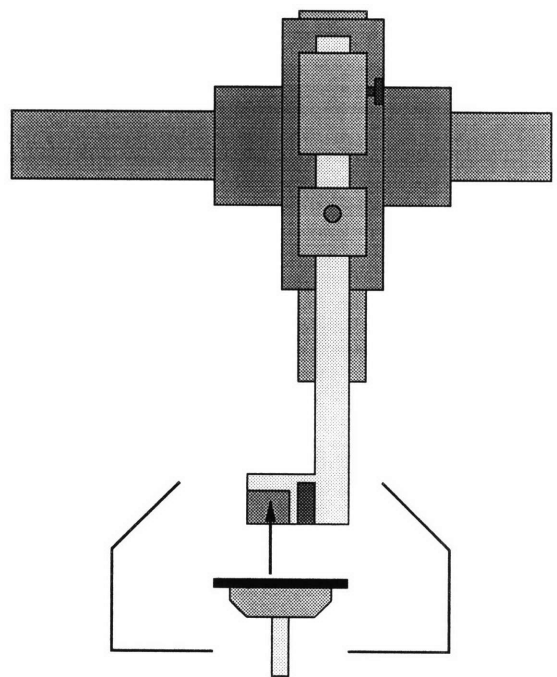
(d) End of cycle

Figure 3-4: Extrusion coating operation.

Chapter 4

Process Variables for Extrusion-Spin Coating Method

4.1 Selection of process variables

There are numerous process variables in extrusion-spin coating. However, each process variable has to theoretically evaluated because experimental determination of the consequences of each is almost impossible. In the following sections, process variables and their theoretically determined significances are listed for both extrusion-slot coating and spin coating processes.

4.2 Process variables for extrusion-slot coating

4.2.1 Background

According to the literature search, process variables that affect extrusion-slot coating are:

1. Gap distance.

2. Coating speed.

3. Dimensions of extrusion head.

4. Properties of coating fluid.

Choinski [7] analyzed the relations between bead coatability and coating parameters. He asserted that bead formation dynamics is the key in slot coating and enumerated factors that are closely related to the dynamics. Equation 4.1 shows the relationship of bead coatability and those parameters:

$$Bead\ coatability \propto Kh/\mu V_{sub}d \tag{4.1}$$

where, K is the coating factor, h is the wet thickness, μ is the fluid viscosity, V_{sub} is the coating speed, and d is the gap distance between the extrusion head and substrate. Coatability represents how much area has been coated and how uniform the coated area is. The relationship reveals much useful information. The fact that thicker wet coating gives easier and better coating is self-evident since thicker wet thickness means more resist has been applied. Liquid with lower viscosity tends to spread out more smoothly and thus results in better coating. Unpredictable fluid dynamics occurs at high coating speed, lowering coatability. The same applies at large gap distances. A large gap distance usually causes neck-ins of extruded flow which, again, lead to unstable fluid dynamics. However, this relationship doesn't indicate the quantitative effect of each variable. For example, doubling the wet thickness and coating velocity doesn't necessarily guarantee the same coatability.

Figure 4-1 and Figure 4-2 show a schematic diagram and the important dimensions of extrusion-slot coating, respectively. Most process variables are not independent of one other. A detailed explanation of individual process variables and their interrelations is presented with in following sections.

4.2.2 Gap distance

Gap distance is the distance between the extrusion head and substrate. It is also one of main parameters that distinguish the curtain coating process from the extrusion-slot coating process.

Choinsky [7] emphasizes the importance of the drawdown ratio, DR, in extrusion-
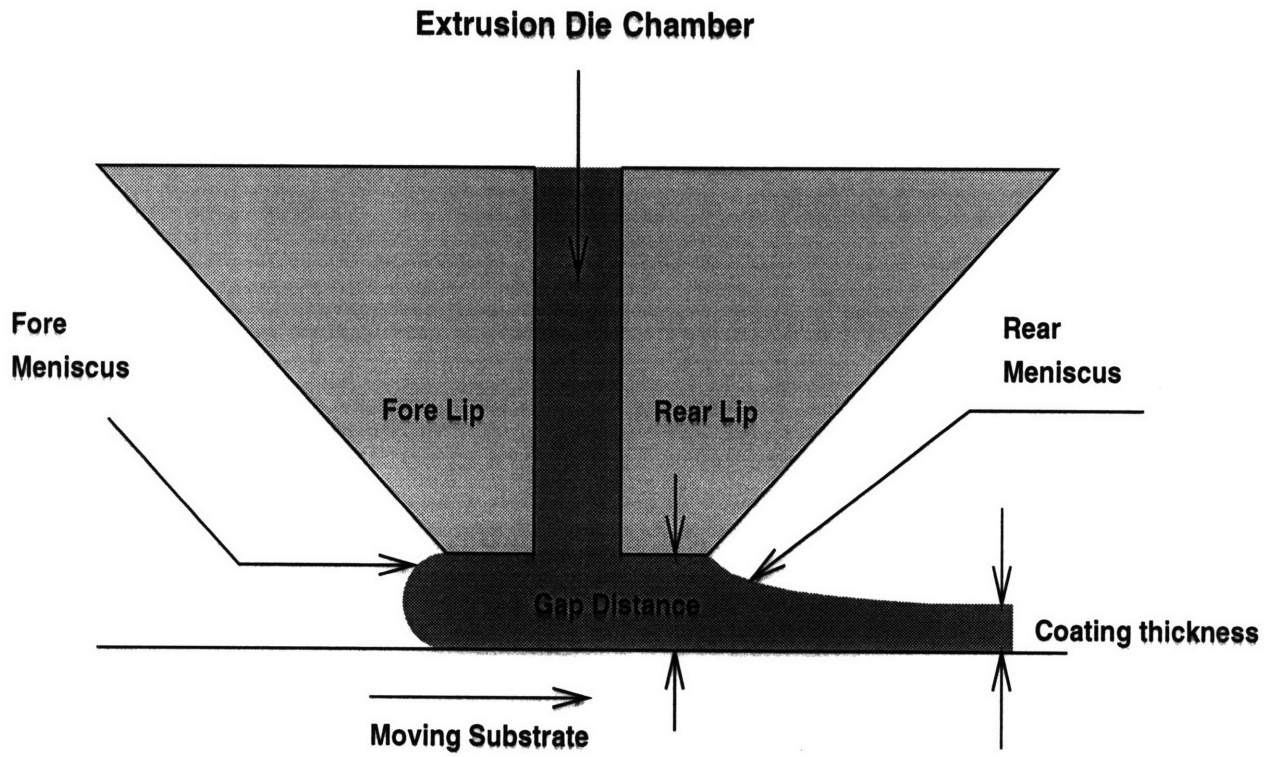
Figure 4-1: Cross-sectional perspective of extrusion-slot coating.
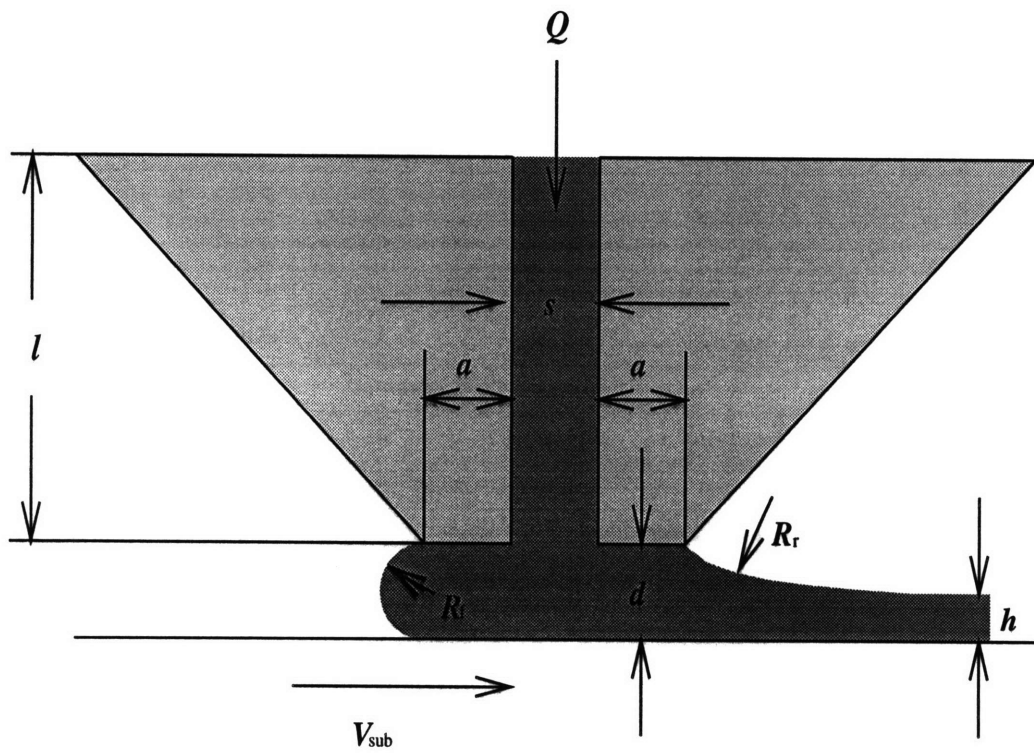
Figure 4-2: Dimensional parameters of extrusion-slot coating.

slot coating, which indicates the ratio of gap distance, d, to wet coating thickness, h. Once stable coating is reached, drawdown occurs uniformly along the extrusion head. If the drawdown ratio has been increased (i.e., the gap distance has been doubled to 2d) the fluid must be drawn down twice as much. However, internal viscous forces prevent the fluid from maintaining linear drawdown and some portion of fluid starts to draw down laterally, creating discontinuities along the extrusion head. As a result, stripes are formed in the coating due to discontinuities in the fore bead. When the drawdown ratio is reduced, the bead remains stable and the coating thickness, h, is unchanged. Even if the extrusion head is skewed, the coating thickness remains constant along the length of extrusion head because the flow remains mainly in the direction of coating.

4.2.3   Coating speed

Coating speed is a process variable which is directly related to production rate. Higher coating speed is desirable to increase the production rate but it can cause instabilities in coating and thus is not desirable from the coating quality aspect. The range of coating speed in which defect-free coating exists must be determined for each type of resist used.

According to theoretical analyses by Ruschak [21], the range of coating speed can be predicted by two algebraic inequalities. These inequalities are expressed in two dimensionless groups: the Beguin number, Be, and the Lewis number, Le:

$$Be + \frac{L_{Ca}}{d}(1 + cos\theta_s) \geq 1.388 Le^{\frac{2}{3}} \geq Be - \frac{L_{Ca}}{d}(1 - cos\theta_s) \tag{4.2}$$

In the absense of a pressure difference between fore meniscus and rear meniscus, Equation 4.2 reduces to the single inequality condition:

$$\frac{L_{Ca}}{d}(1 + cos\theta_s) \geq 1.388 Le^{\frac{2}{3}} \tag{4.3}$$

Combining Equation 4.3 with Equation 2.8 gives:

Table 4.1: Properties of experimental liquids used by Tallmadge *et al.*

	Density (Kg/m^3)	Viscosity $(mPa \cdot sec)$	Surface Tension (N/km)
Liquid 1	1180	22	39.4
Liquid 2	865	68	34.1
Liquid 3	902	281	33.6

$$V_{upper} = \left(\frac{Q(1 + cos\theta_s)}{1.338wd}\right)^{\frac{3}{5}} \left(\frac{\sigma}{\nu}\right)^{\frac{2}{5}} \qquad (4.4)$$

Tallmadge *et al.* [24] have compared experimental results with Ruschak's theoretical model. Using three different liquids whose properties are shown in Table 4.1, Tallmadge *et al.* acquired the operable range of the coating speed. The lower limit of the coating speed has been referred to as the "drip point" at which the bead becomes too large to be maintained between the extrusion die and the substrate and thus results in coating instability. The upper limit has been referred to as the "split point" at which the amount of the fluid bridging the extrusion die and the substrate becomes less than is required to maintain the bead and the uniformity of the coating.

Their experimental data shows that Ruschak's theoretical analysis is a good approximation method for determining the upper and lower coating speed limit except for one process variable. The gap distance does not affect the result as predicted by the theoretical model. Ruschak's inequality is a good approximation method to predict the tendency of the bead coating stability.

Another constraint for maximum coating speed limit is air entrainment. Deryagin and Levi [10] were the first to note that the dynamic contact angle increases proportional to coating velocity. When the dynamic contact angle reaches 180°, the air film carried along by the moving substrate causes incomplete wetting, resulting in air entrainment. Perry [20] correlated the Weber number with the Reynolds number as:

$$We = 0.196Re^{0.83} \qquad (4.5)$$

Both Weber number and Reynolds number contain the characteristic length, L, which is the distance between the static and the dynamic contact lines.

Burley and Kennedy [4, 5, 6] correlated the velocity of air entrainment as:

$$We = 0.834Re^{0.80} \tag{4.6}$$

As the characteristic length, L, is not known beforehand, Burley and Kennedy[4, 6] obtained an equally good correlation with:

$$V_{180} = 67.7\left[\mu\left(\frac{g}{\rho\sigma}\right)^{0.5}\right]^{-0.67} \tag{4.7}$$

Joos et al. [15], and Mues et al. [19] predicted that air entrainment begins when the contact angle reaches 180°. Mues explained that the contact angle, θ, increases with the capillary number, $Ca = \frac{\mu V}{\sigma}$, and air entrainment begins when capillary number reaches the value of 0.25. Thus the coating speed at which air entrainment begins can be derived as:

$$V_{air\ entrainment} = \frac{\sigma}{4\mu} \tag{4.8}$$

The maximum coating speed should be less than $V_{air\ entrainment}$.

A theoretical window of coatability using Ruschak's inequality, Burley's approximate correlation, and Mues' relation was established in this project as shown in Figure 4-3. Two different resists (AZ1512 and AZ Deep UV resist) whose properties are listed in Table 4.2 were used to estimate the maximum coating speed. The window of coatability is the overlapping region below each plottings. From Figure 4-3, it can be seen that the window of coatability for AZ Deep UV resist is broader than the one for AZ1512 resist due to the lower viscosity of the former.

4.2.4 Dimensions of extrusion head

The internal geometry of the extrusion head affects the pressure drop created across the internal die. Equation 4.9 illustrates that when the path is rectangular, the
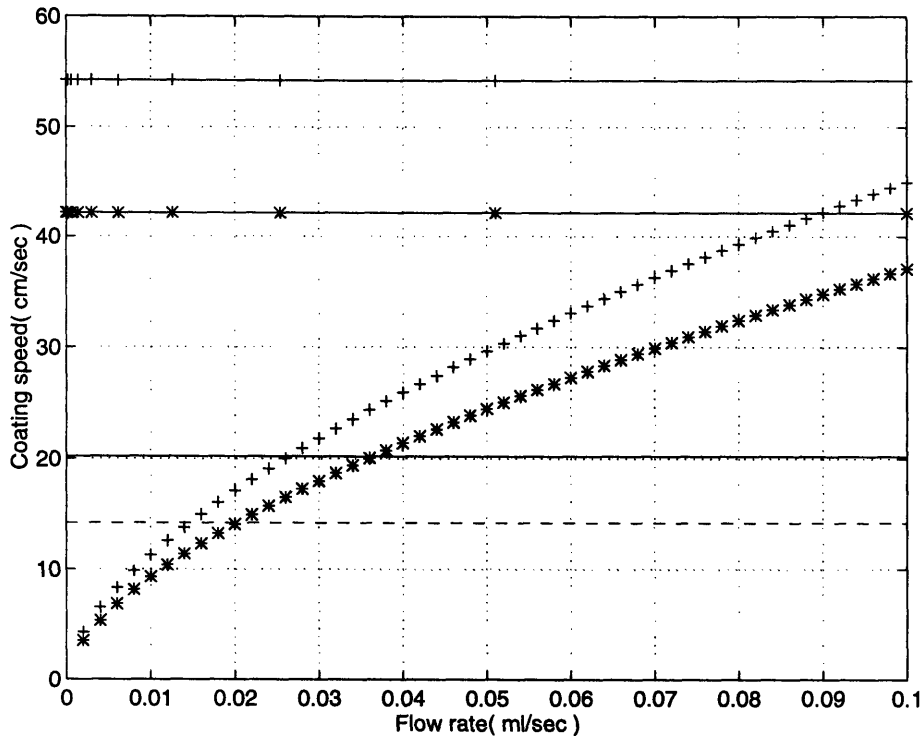
Figure 4-3: Theoretical window of coatability. "*" and "+" indicate Ruschak's inequality. "+-" and "*-" indicate air entrainment speed by Mues. Continuous line and dotted line indicate Burley's approximate correlation. "*", "*—", "- -" : AZ1512 resist, "+", "+—", "–": AZ Deep UV resist.

pressure drop, ΔP, varies proportionally to the flow rate, Q, the kinematic viscosity of the coating liquid, ν, and the path length, l, and inversely proportional to the cube of the slit length, s.

$$\Delta P = \frac{12\nu l Q}{s^3} \tag{4.9}$$

The pressure drop should remain within a reasonable range to maintain a stable flow rate for the coating liquid.

4.2.5 Properties of the coating fluid

We have conducted experiments with two different types of photoresist. The properties of each are shown in Table 4.2. The density of each photoresist is closely related to its solid content. Light sensitive polymeric materials are the main components of solid content. The remaining photoresist consists of solvent, which evaporates after

Table 4.2: Properties of two different photoresists.

Photoresist used	Specific Density (Kg/m^3)	Viscosity $(mPa \cdot sec)$	Surface Tension (N/km)
AZ1512	1040	19	32
AZ1200P	1000	11	30

the coating. The volume fractions of the solid content and solvent play an important role in determining the viscosity and surface tension of photoresist.

Viscosity

The viscosity of a photoresist depends upon the solids content and the temperature. Viscosity plays an important role in determining the maximum coating speed and the flow rate as discussed in the previous section. Equations 4.4 and 4.8 predict that the maximum coating speed and flow rate can be increased by using a less viscous liquid. Viscosity is also one of two key parameters that determine the thickness of a deposited film in the spin coating process, the other being the spin speed [25].

Choinsky [7] stated in his article that once the coating bead has been established, the viscosity of coating fluid does not affect the equilibrium wet thickness. However, he emphasized that the viscosity, along with other parameters, is the critical process variable in determining the formation of a well-shaped bead.

Surface tension

Surface tension is a property affecting the coating result. All sorts of defects are directly or indirectly caused by surface tension. Gutoff and Cohen [14] have illustrated many surface-tension-driven defects.

Surface tension is directly related to wettability of a coating liquid since wettability is represented by the sum of forces at the edge of wet coating, as in Figure 4-4.

The Young-Laplace equation illustrates the relationships between pressure drop between interfaces, surface tension, and radii of curvature for the curved surface:
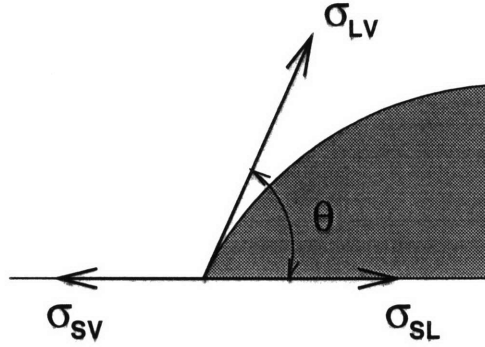
Figure 4-4: Surface forces at the edge of a wet coating

$$\Delta P = \sigma \left(\frac{1}{r_1} + \frac{1}{r_2} \right) \tag{4.10}$$

In a cylindrical surface such as a coating bead, $r_2 \to \infty$ leaves:

$$\Delta P = \frac{\sigma}{r_1} \tag{4.11}$$

Higher pressure on the concave side of the interface is called capillary pressure. It plays an important role in forming the shape of the coating bead.

Surface tension can cause many defects in the extrusion coating process. As our prime goal is to establish the window of defect-free regions for the process variables, thorough investigation of possible defects due to surface tension has to precede and such regions should be avoided during the extrusion coating process.

Gutoff [12] clearly explains defects caused by surface tension and their behavior. The most common defects were illustrated in Chapter 2. Additional information on them is:

Ribbing

Bixler [3] described the ribbing in slot coating using a finite element analysis technique. He reported that the following factors induce ribbing: high capillary number $Ca = \frac{\mu V_{sub}}{\sigma}$, low drawdown ratio $DR = \frac{d}{h}$, low Reynolds number $Re = \frac{\rho d V_{sub}}{\mu}$. Therefore, to decrease the risk of ribbing:

1. Lower the viscosity of coating fluid.

2. Decrease coating speed.

3. Increase surface tension.

4. Increase wet thickness.

5. Decrease the gap distance between head and substrate.

Chatter

Chatter is sometimes called barring because it appears as crossweb bars of fairly uniform width and period. In almost all cases, it is caused by mechanical vibration. The system must isolate the coating subsystem from any sort of vibrations to eliminate chatter.

Chatter can also occur near the limits of coatability. In such case, slowing down the coating speed, decreasing the gap distance, or increasing the vacuum can help resolve the instability.

Streaks

Streaks are not considered as instability. Nevertheless, they are ought to be studied carefully since they result in coating defects, too. Streaks can be caused by:

1. Particles caught in the exit of slot coater.

2. Particles carried by the substrate into fore meniscus.

3. Particles or bubbles remaining in extrusion die.

4. Nicks in extrusion head.

To achieve a good coating, it is essential to keep particles from the coating flow. Photoresist has to be filtered before it reaches the coating head. Bubbles in supplying line have to be removed, and the substrate must be free of dirt. Nicks can be removed by hand with a whetstone. However, stoning out the extrusion head will round the

Figure 4-5: Fat edges

edge. According to Zimmerman and Fahrni [26], the radius of the coating edge should be less than 50 μm to pin down the bead, which will otherwise create chatter. Thus, great caution must be exersized in removing nicks from the extrusion head.

Fat Edges

Fat edges are sometimes called "picture frames." Because the coating edges is thinner than the rest with the approximately same evaporation rate, concentration will increase faster at the edges. As a consequence, the edge surface tension will be higher than the middle and it will cause a flow toward edges, creating fat edges.

4.3 Process variables for spin coating

4.3.1 Delay time

Delay time is the time gap between the end of extrusion coating and the start of spin coating. Delay time becomes more and more important as the viscosity of the fluid decreases. Less viscous fluids tend to wet better than more viscous fluids and thus the disappearance rate of the overlap and pool of resist at the center is much faster with a less viscous resist. With a longer delay time, the coating liquid can spread out more and form a more uniform film. However, delay time is constrained by the demand for higher production rate and thus must be optimized.

4.3.2 Spin speed

Spin speed is the angular velocity at which a wafer is spun for a specific time. Spin speed mainly contributes to forming a certain film thickness. The angular velocity between 3000 and 5000 rpm is used to attain 1 μm thickness. The experiments of Daughton and Givens [9] show that the thickness of photoresist is approximately proportional to $\Omega^{1/2}$. Sukanek [23] collected the existing data and made the best fit line for evaluation of coating thickness with regard to spin speed. The thickness of each resist has been normalized by the measured thickness h_R at some reference speed Ω_R. The best fit line was derived as:

$$\frac{h}{h_R} = 0.987(\frac{\Omega}{\Omega_R})^{-0.504} \tag{4.12}$$

Meyerhofer [17] developed a rough model for estimating the required time for the spin-off stage. He assumed that there is no evaporation during the spin-off stage since the time is short enough. He also assumed an imaginary stage at which all the evaporation takes place, called the "evaporation stage." Times for spin-off and evaporation stages are represented in Equation 4.13 and Equation 4.14, respectively:

$$t_{spin\ off} = \frac{3\mu_0}{4\rho\Omega^2} \left(\frac{1}{h^2_{spin\ off}} - \frac{1}{h_0^2} \right) \tag{4.13}$$

$$t_{evaporation} \equiv \frac{V_{solvent}}{e} = h_{spin\ off}\frac{\rho^0_{sol}}{\rho e} \tag{4.14}$$

The final thickness of the film can be expressed as:

$$h_f = \left(1 - \frac{\rho^0_{sol}}{\rho} \right) h_{spin\ off} = \left(1 - \frac{\rho^0_{sol}}{\rho} \right) \frac{3\mu_0 e}{[2\rho\Omega^2(\rho^0_{sol}/\rho)]^{1/3}} \tag{4.15}$$

Total time–excluding the short deposition and spin-up stages–to reach the final thickness would simply be:

$$t = t_{spin\ off} + t_{evaporation} \tag{4.16}$$

Chapter 5

Design of Experiments

5.1   Preparation for experiments

The window of coatability was established theoretically before the experimentation. Figure 5-1 illustrates the region in which extrusion-slot coating remains stable. The maximum coating speed is plotted versus various wet thicknesses. Stars and circles indicate experimental data points of AZ Deep UV and AZ1512 resist, respectively. The lower bound was attained by correlating coating speeds with different wet thicknesses at a constant minimum flow rate.

5.2   Process plan

Since the ultimate goals of this thesis are establishing windows of coatability with various process variables and optimizing the process variables, the following observations were essential to the experiments.

1. The maximum wet coverages over a range of different coating speeds at several coating gaps and different flow rates.

2. The minimum wet coating thickness with neither solvent saturated atmosphere nor bead vacuum.
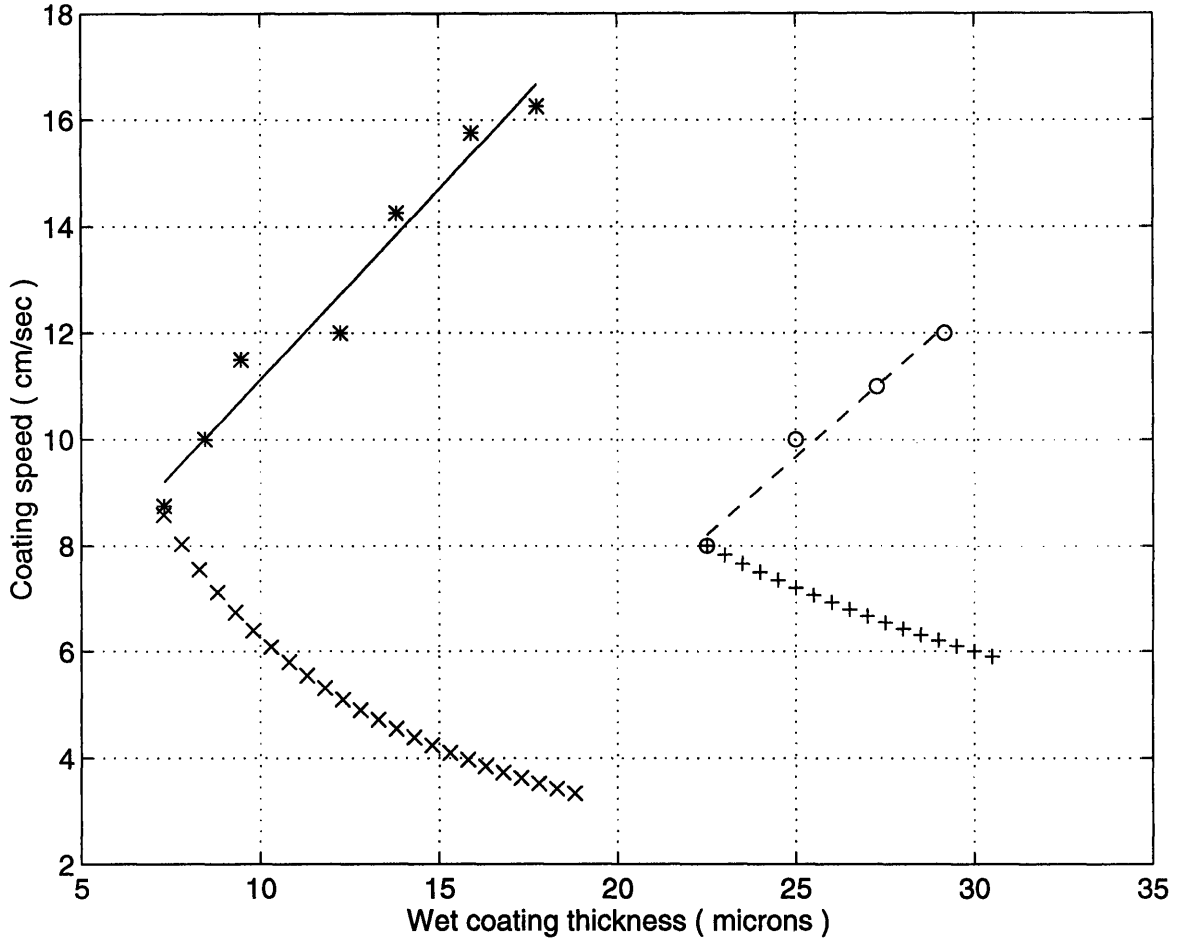
Figure 5-1: Window of coatability for two different types of photoresist. Upper bound was set by determining maximum coating speed corresponding to different coating thicknesses: maximum speed of Deep UV resist (*), maximum speed of AZ1512 (o). Lower bound was set by using the relationship between wet thickness and coating speed at constant flow rate: "x": lower bound for AZ Deep UV resist, "+": lower bound for AZ1512 resist.

Temperature and humidity have to be recorded for every experiment. Humidity has an huge influence on the evaporation of coating liquid during the extrusion-slot coating process and temperature affects the uniformity of overall coating after the spin coating process.

Assessing the rate of evaporation is very difficult yet very important for the experiments. Since most of the extruded flow forms a coating film with a width of about 2 cm and a thickness less than 50 μm, the evaporation rate is tremendously high. The effect of evaporation has to be properly isolated to determine the effects of other process variables.

Estimation of neck-in is another important issue. Neck-in has to be exactly estimated to determine the point at which the minimum amount of overlap occurs, not to mention to assign the right amount of overlaps for experiments. Calibration of neck-ins is discussed in Appendix B.

5.3 Design of experiments

Experimental points were selected within the window of coatability and initial experiment conditions were selected to determine critical process variables in addition to testing the feasibility of extrusion-spin coating. The initial experiments are indicated in Table 5.1.

In all experiments, coating speed, V_{sub}, represents the linear velocity of the extrusion head in a tangential direction to the wafer. The wet thickness, h, represents the initial wet coating thickness. The spiral coating time, t_{spiral}, includes two discrete times: dispense time and center spread time. Dispense time corresponds to a time period during which dispense has been triggered on and off. Dispense time is usually equivalent to coating time but sometimes, the extrusion head is moved after the end of dispense to smoothen the pool of resist at the center. The time period from the end of dispense to raising of the extrusion head is the center spread time. Note that coating time does not include delay time. Disp. Vol. stands for the total dispense volume.

First and second sets of experiments were designed to find the optimal conditions for successful coating with AZ1512 and AZ Deep UV resist as illustrated in Table 5.2 and Table 5.3, respectively.

The prime target of these experiments is to determine critical process variables. Many process variables are involved in the extrusion-spin coating, as enumerated in Chapter 4. However, some parameters can be critical while others are negligible in their contributions to coating uniformity. It is very important to weed out these less important process variables and identify the critical ones.

To test the influence of process variables among those selected ones, results must be measured by means and standard deviations. Standard deviation will represent uniformity while mean will be the desired coating thickness. For each experiment, spin coating with 25 *ml* center dispense has been conducted to establish a bench mark. This bench mark is the highest standard achievable with the experimental spin coater. Comparison between the results of extrusion-spin coating with a bench mark will establish a target uniformity for the extrusion-spin coating method.

Table 5.1: Experimental setup with AZ1512 resist.

Exp. No.	Coating Speed (cm/sec)	Wet Thickness (μm)	Flow Rate (ml/sec)	Coating Time (sec)	Disp. Vol. (ml)
1	8.25	42.4	0.07	29.3	2.051
2	8.25	42.4	0.07	29.4	2.058
3	8.25	42.4	0.07	29.5	2.065
4	8.25	42.4	0.07	29.6	2.072
5	8.25	42.4	0.07	29.8	2.086
6	8.25	42.4	0.07	30.0	2.100
7	8.25	42.4	0.07	29.5	2.065
8	12.0	29.2	0.07	20.1	1.407
9	10.0	35.0	0.07	24.0	1.680
10	10.0	35.0	0.07	24.1	1.687
11	10.0	35.0	0.07	24.2	1.694
12	10.0	35.0	0.07	24.3	1.701
13	10.0	35.0	0.07	24.5	1.715
14	10.0	35.0	0.07	24.7	1.729
15	10.0	35.0	0.07	24.0	1.680
16	10.0	35.0	0.07	24.1	1.687
17	10.0	35.0	0.07	24.2	1.694
18	10.0	35.0	0.07	24.3	1.701
19	10.0	35.0	0.07	24.5	1.715
20	10.0	35.0	0.07	25.0	1.750
21	10.0	35.0	0.07	25.5	1.785
Note : From experiment 1 to 10, 5 sec delay time was applied. After experiment 11, 7 sec delay time was applied.					

Table 5.2: Experimental setup with AZ1512 resist.

Exp. No.	Coating Speed (cm/sec)	Wet Thickness (μm)	Flow Rate (ml/sec)	Coating Time (sec)	Disp. Vol. (ml)
1	8.0	23.9	0.037	30.1	1.114
2	8.0	23.9	0.037	31.7	1.173
3	8.0	25.0	0.039	30.0	1.170
4	8.0	25.0	0.039	31.5	1.229
5	10.0	25.0	0.048	24.2	1.162
6	10.0	25.0	0.048	25.5	1.210
7	6.0	29.2	0.035	39.2	1.372
8	6.0	29.2	0.035	41.2	1.442
9	8.0	29.2	0.046	29.7	1.336
10	8.0	29.2	0.046	31.3	1.440
11	10.0	29.2	0.057	23.9	1.362
12	10.0	29.2	0.057	25.2	1.436
13	12.0	29.2	0.068	20.1	1.367
14	12.0	29.2	0.068	21.3	1.448
15	6.0	35.0	0.042	38.9	1.634
16	6.0	35.0	0.042	40.1	1.684
17	8.0	35.0	0.055	29.5	1.623
18	8.0	35.0	0.056	31.0	1.736
19	10.0	35.0	0.069	23.7	1.635
20	10.0	35.0	0.070	25.0	1.750

Note : From experiment 1 to 6, 60 μm gap distance has been used.
After experiment 7, gap distance of 80 μm has been used.
Acceleration of 5000 rpm/sec has been used for all experiments.
No delay time was introduced.

Table 5.3: Experimental setup with AZ Deep UV resist.

Exp. No.	Coating Speed (cm/sec)	Wet Thickness (μm)	Flow Rate (ml/sec)	Coating Time (sec)	Disp. Vol. (ml)
1	11.0	9.9	0.021	21.7	0.441
2	11.0	9.9	0.021	22.0	0.447
3	11.0	9.9	0.021	22.3	0.454
4	10.0	10.0	0.020	23.9	0.450
5	10.0	12.5	0.024	23.9	0.562
6	8.0	15.0	0.024	29.9	0.676
7	10.0	15.0	0.029	23.9	0.675
8	12.0	15.0	0.035	20.0	0.676
9	14.0	15.0	0.041	17.1	0.677
10	8.0	17.5	0.027	29.9	0.788
11	10.0	17.5	0.034	23.9	0.787
12	12.0	17.5	0.041	20.0	0.788
13	14.0	17.5	0.048	17.1	0.790
14	16.0	17.5	0.055	15.0	0.788
15	8.0	20.0	0.031	29.9	0.901
16	10.0	20.0	0.039	23.9	0.899
17	12.0	20.0	0.047	20.0	0.901
18	14.0	20.0	0.055	17.1	0.903

Note : Gap distance of 40 μm has been used for all experiments.
Acceleration of 5000 rpm/sec has been used for all experiments.
No delay time was introduced.

Chapter 6

Results and Discussion

6.1   Experimental results and analysis

The following sections will evaluate extrusion-spin coating, identify the effect of each process variable, and optimize the process variables. Evaluation of extrusion-spin coating will verify the feasibility of the method. Once the effect of each process variable is experimentally identified, it will be compared with theoretical estimations. Only the significant ones will be considered in designing experiments in the future. Finally, optimization of process variables will be conducted by analyzing experimental data.

6.1.1   Evaluation of extrusion-spin coating

Experiments to evaluate the extrusion-spin coating method has been designed in Table 5.1. Figure 6-1 illustrates the results of extrusion-spin coating in comparison to conventional spin coating. Uniformities of extrusion-spin coating surpass that of spin coating despite the smaller amount of total dispense. The sudden increase of standard deviation in the experiment number 11 was caused by an extra 2 seconds delay time. The width of coating was nearly 2 cm, which is extremely wide compared to the wet thickness of about 40 μm. This wide yet thin coating film causes the solvent in the coating liquid to evaporate very quickly, resulting in uneven spread

62
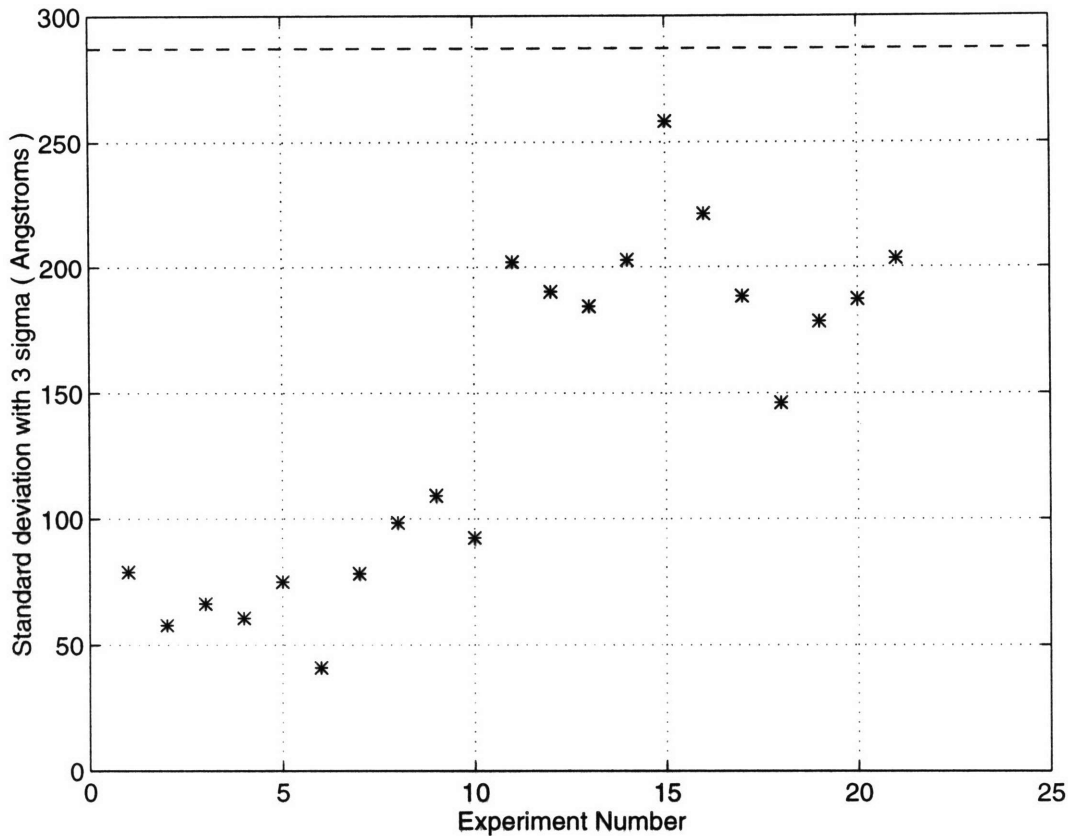
Figure 6-1: Standard deviation of coating uniformity for AZ1512 resist. Dotted line represents standard deviation with 5 *ml* dispense of resist as a bench mark.

during the spin coating stage.

Despite the effect of the evaporation, all data points remained within a region in which the coating uniformity is better than that of the spin coating method. In conclusion, Figure 6-1 illustrates the strong potential for the successful industrial application of the extrusion-spin coating method.

6.1.2 Appraisal of effect of gap distance

Maximum coating speed was first investigated by varying flow rate and gap distance. Table 6.1 shows the result. It indicates that the maximum coating speed is not affected by varying gap distance. The bead became very unstable once the maximum gap distance had been exceeded, which implies that as long as the critical drawdown ratio is not exceeded, the coating will remain stable regardless of the gap distance. This phenomenon can be explained by neck-ins of extruded flow. Figure B-2 and

63

Flow rate	Gap Distance (μm)		
(ml/sec)	40	80	120
0.036	8.0	8.0	8.0
0.05	10.0	10.0	10.0
0.06	11.0	11.0	11.0
0.07	12.0	12.0	12.0

Table 6.1: Maximum coating speed (cm/sec) with different gap distances for AZ1512 resist.

Figure B-3 in Appendix B indicate the maximum gap distances and corresponding drawdown ratios. Maximum gap distance is restrained by the sudden increase of neck-in as gap distance broadens. A detailed explanation of the neck-in is presented in Appendix B.

6.1.3   Experimental data

All the uniformity data were retrieved by a density mapping device. Figure 6-2 illustrate the three dimensional mapping result with AZ1512 resist. The edges of the wafer show positive deviation from the mean. Resist applied at the edges dried out first and as a result, did not spread during the spinning stage. The peak formed in the center region comes from the excess dispense on the center. Figure 6-3 illustrates the spin coating results using the same resist. One side of the edge has minus deviation from the mean because of the center dispense method. Resist was not applied from the outer edge to the center and therefore the evaporation rate at the edges were not as high as the extrusion-spin coating method.

Figure 6-4 illustrates the two dimensional mapping result with AZ Deep UV resist. Again, the edges of the wafer show positive deviation because of the high evaporation rate. The center shows negative deviation which means an insufficient amount of resist has been applied on the center region. The thick line near the edge represents the mean thickness at which deviation is zero. Figure 6-5 illustrates the spin coating results using AZ Deep UV resist.

Standard deviations from mean values are measured to represent the coating uni-
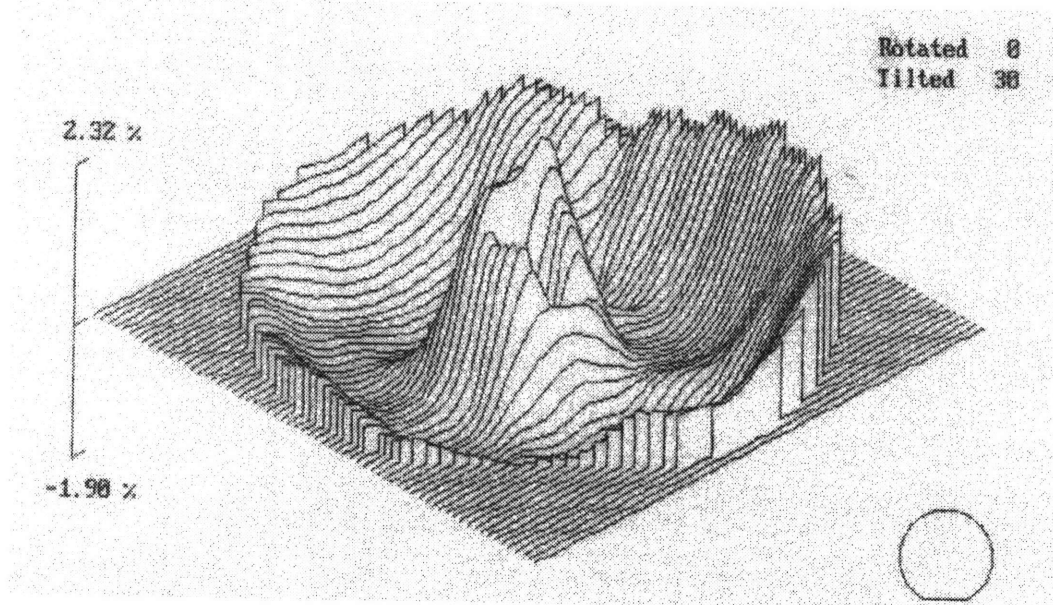
Figure 6-2: 3D-mapping of extrusion-spin coating result using 1.72 ml dispense of AZ1512 resist. Mean: 1.4428 μm, Standard deviation with 3σ: 112.72 Å.

formity. Data obtained with AZ1512 and AZ Deep UV resist are plotted in Figure 6-6 and Figure 6-7, respectively.

6.1.4   Optimization of process variables

Optimization of process variables cannot be conducted correctly in an uncontrolled environment because of the dominating effect of evaporation on the coating. Figure 6-2 and Figure 6-4 show that a thicker coating is always formed on the edge. Experimental results in Figure 6-6 and Figure 6-7 also indicate that thicker initial wet thickness and low coating time always result in better uniformity. The effect of evaporation has to be excluded to evaluate the actual effect of each process variable. A solvent saturated atmosphere is essential to isolate the evaporation problem.

Figure 6-3: 3D-mapping of conventional spin coating result using 25 *ml* dispense of AZ1512 resist. Mean: 1.4627 *μm*, Standard deviation with 3σ: 109.46 Å.

Figure 6-4: 2D-mapping of extrusion-spin coating result using 0.903 *ml* dispense of AZ Deep UV resist. Mean: 0.7200 *μm*, Standard deviation with 3σ: 80.22 Å.
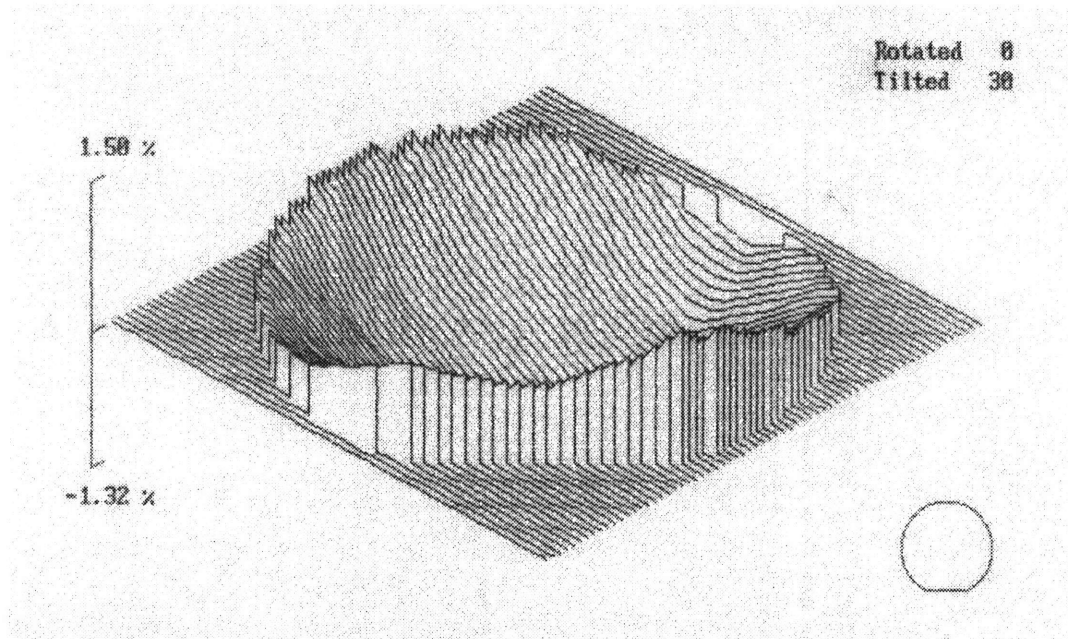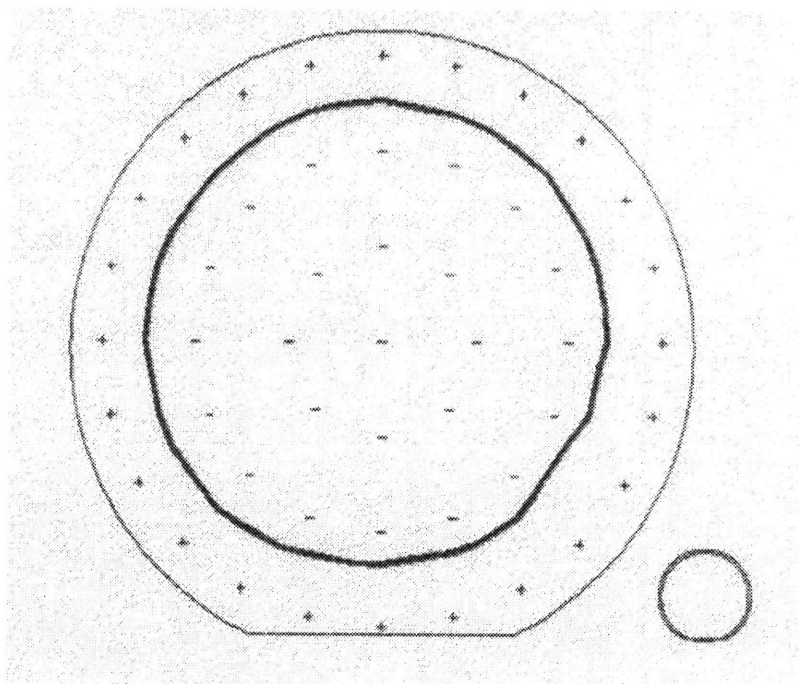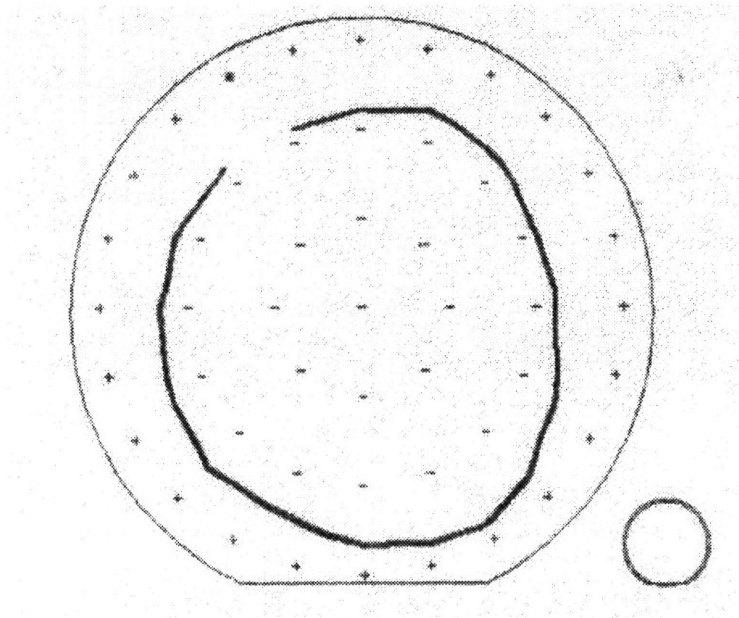
Figure 6-5: 2D-mapping of conventional spin coating result using 25 *ml* dispense of AZ Deep UV resist. Mean: 0.7277 μm, Standard deviation with 3σ: 24.99 Å.

6.2 Experimental observations

1. Gap distance doesn't influence coating much unless it exceeds a critical value to be in curtain coating region.

2. The extrusion head must go over the center perfectly to prevent bubbles forming at the center.

3. The amount of resist applied onto center has to be carefully manipulated to avoid center defects.

4. When using viscous liquid, wetting can be difficult, which leads to gaps between two streams of resist and thus coating errors.

5. Delay time should not exceed certain limits since evaporation takes place so quickly that resist near the edge tends to solidify and thus not spread in the spin coating stage, which causes thicker coating on edges of wafer.

Figure 6-6: Standard deviation of coating uniformity for AZ1512 resist. Dotted line represents standard deviation with 25 *ml* dispense of resist for a bench mark.

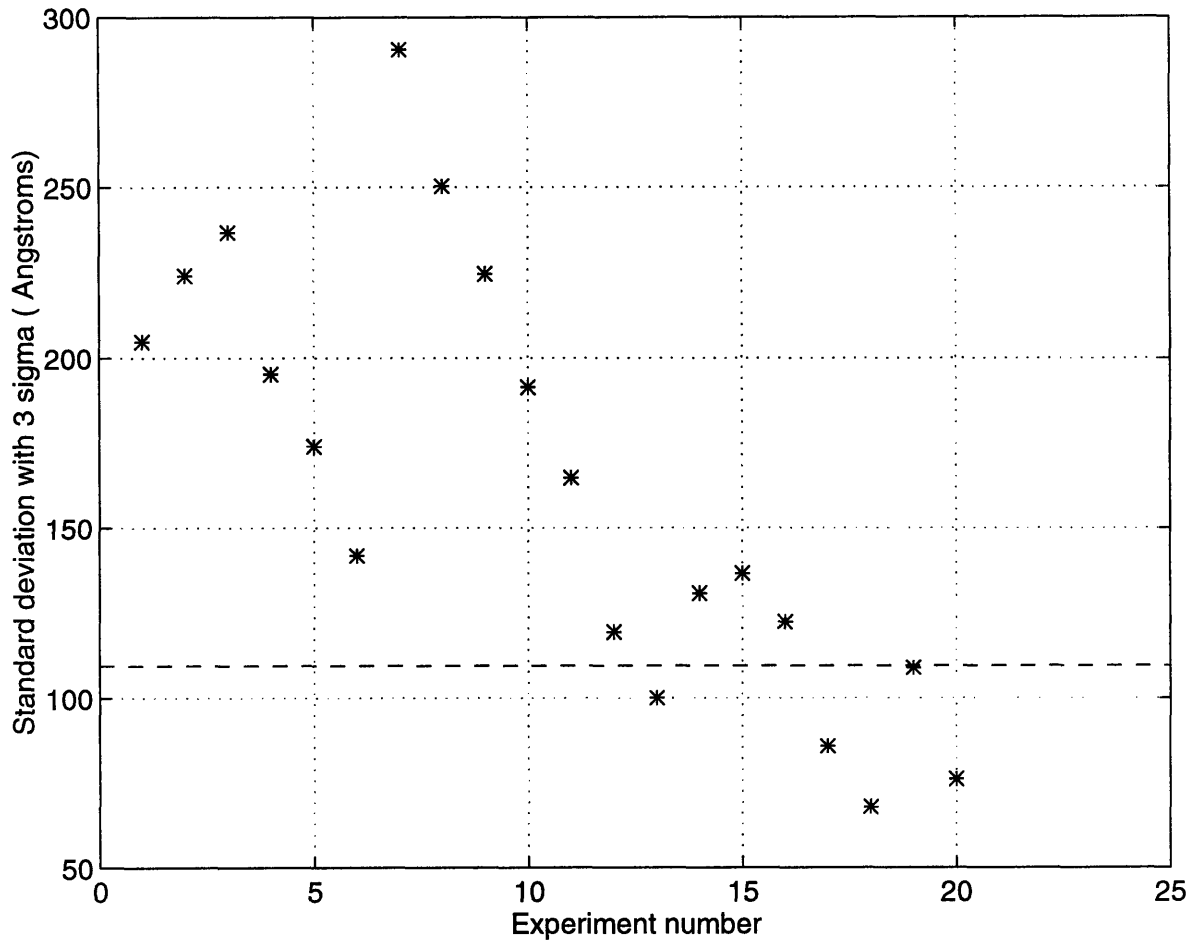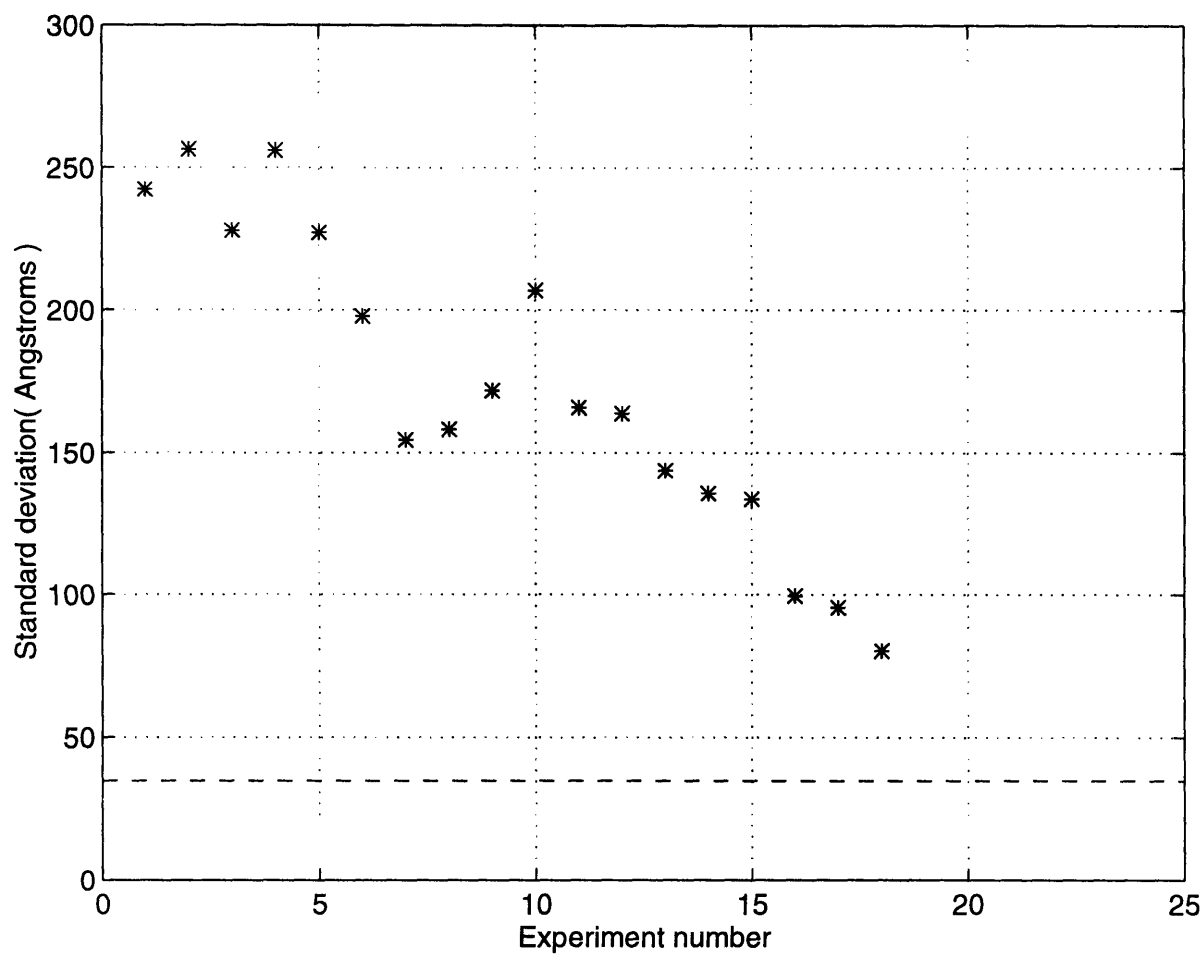Figure 6-7: Standard deviation of coating uniformity for AZ Deep UV resist. Dotted line represents standard deviation with 25 *ml* dispense of resist for a bench mark.

6. Whenever a bubble is entrapped in the center, strips of solidified photoresist were detected in the pool of resist in the center. These strips are found with the extrusion-slot coating. When bubbles are present in the center, the number and length of strips augments distinguishably.

7. Bubbles from the pump must be eliminated.

8. Hose compliance and resistance in hose and extrusion head prevent the anticipated amount of dispense. Pump has to be calibrated more accurately to estimate the amount of dispense.

9. Evaporation of coating liquid must be retained until the spin coating stage to eliminate striations at the end of the coating cycle.

10. The effect of overlap between joining streams is negligible in final coating uniformity.

11. Center problems are noticeably reduced with less viscous fluid.

12. Evaporation influences coating uniformity dominantly when initial wet coating thickness is less than 20 μm for AZ Deep UV resist.

6.3   Discussion

There are certain problems with the current extrusion-spin coating method. The most critical problems are:

1. Center problem.

2. Evaporation.

3. Run-out of chuck.

The center is always a critical region in which the behavior of coated flow is unpredictable. However, the center became less of a problem as the viscosity of the coating flow was lowered due to the better wetting of the low viscous fluid. The trend of

lowering the viscosities of new resist types will contribute greatly to resolving the center problem.

Another problem is caused by evaporation. Due to the fast evaporation of photoresist, fair uniformity could not be achieved with a wet coating thickness less than 20 μm in uncontrolled atmospheric surroundings. A controlled environment must be created to retard the evaporation rate of the solvent as much as possible.

Run-out of chuck is one of the major problems. Since the response time from the control feedback was not short enough, the gap distance between the extrusion head and substrate was inconsistent during the extrusion-slot coating process. Changing the gap distance can cause the amount of the neck-in to vary and thus cause different overlaps, especially near the extreme points. Feedback control must be improved for better gap distance control and more consistent data.

Chapter 7

Conclusion and Future Work

7.1 Conclusion

The prototype of an extrusion-spin coater has been built and tested. The results of the evaluation corroborate the theoretical prediction of the strengths of the extrusion-spin coating method. Despite some of the problems enumerated in Chapter 6, data from initial experiments imply strong potential for successful application of extrusion-spin coating method. More work has to be done to fine-tune the prototype.

Coating efficiency was definitely higher when compared to the conventional spin coating method. Coating uniformity of 10% was achievable with 25% solids content resist. The highest coating efficiency attained was about 40% with 20% solids content resist.

Coating uniformity was improved and the defect level decreased. The results in Figure 6-6 show that as long as the effect of evaporation can be excluded, uniformity will excel that of the spin coating method. Even with the high evaporation rate, coating uniformity of 80 Å (3σ) was obtained with 0.903 ml dispense.

The coating time has been maintained within the 30 seconds of the spin coating method.

7.2 Future Work

Some problems have been surfaced from the initial experiments with the extrusion-spin coating technique. The prototype must be further modified to add the following:

1. improving the feedback control.

2. replacing the current pump with a more accurate one.

3. installing the vacuum for extrusion-slot coating process.

4. creating a solvent saturated atmosphere for extrusion-slot coating process.

The future work consists of installing four major subsystems. Feedback control has to be improved. Active control has to be adapted to follow an exact desired path regardless of run-out of chuck. The pump has to be replaced with a more accurate one to control the flow rate with higher precision. This should solve the center overlap problem as discussed in Chapter 6.

Vacuum has to be installed for two major reasons:

1. to increse the coating speed.

2. to decrease the wet thickness.

Beguin [2] has used a pressure differential across the bead in a coater to increase coating speed. Lee *et al.* [16] have investigated the effect of vacuum in forming minimum wet thickness in extrusion-slot coating. At lower viscosities, bead vacuum can easily reduce the minimum wet thickness by 20-30%. Since the prototype has no vacuum, installation of a vacuum system will increase the coating speed at the equivalent flow rate and thus decrease wet thickness.

Lastly, a solvent saturated atmosphere has to be created. According to the experiments, the evaporation of the solvent affected the coating result dramatically when the initial wet coating thickness was less than 20 μm. The average humidity recorded for the experiments was between 20-40%. By using solvent atmosphere control, evaporation will be retained at the lowest level during the extrusion coating process, which will lead to a thinner initial coating and thus higher coating efficiency.

Appendix A

Mathematical Analysis of Spiral Motion

The spiral coating pattern was adopted for extrusion-spin coating for it alone can provide a continuous stream of extruded flow on a spinning disk. As a well-formed bead is the most important factor to extrusion-slot coating, maintaining the continuous stream is extremely critical. The extrusion-slot coating and the spiral pattern are shown in Figure 2-12 and Figure 2-15, respectively.

The coating speed, V_{sub} is a function of the radial position, r, and the angular velocity, Ω:

$$V_{sub} = r\Omega \tag{A.1}$$

The velocity in the radial direction is a function of the slit width, w, and the angular velocity, Ω, and can be expressed as:

$$V_r = \frac{w\Omega}{2\pi} = -\frac{dr}{dt} \tag{A.2}$$

with the initial condition, $r = r_0$ @ $t = 0$, where r_0 is the initial start position and equals $R + w$.

Integrating Equation A.2 for the radial position, r, gives:

$$r = \sqrt{r_0{}^2 - \frac{wV_{sub}}{\pi}t} \qquad (A.3)$$

By substituting r in Equation A.1 by r in Equation A.3, the angular velocity can be obtained as:

$$\Omega = \frac{V_{sub}}{\sqrt{r_0{}^2 - \frac{wV_{sub}}{\pi}t}} \qquad (A.4)$$

Substituting Ω in Equation A.2 with Ω in Equation A.4 gives the radial velocity, V_r:

$$V_r = \frac{wV_{sub}}{2\pi\sqrt{r_0{}^2 - \frac{wV_{sub}}{\pi}t}} \qquad (A.5)$$

Total time for the spiral coating can be obtained by solving Equation A.3 for t:

$$t_{spiral} = \frac{\pi(r_0{}^2 - r_f{}^2)}{wV_{sub}} \qquad (A.6)$$

where r_f is equal to the slit width.

Appendix B

Experimental Data of Neck-Ins and Corresponding Maximum Gap Distances

Neck-in is the behavior of a fluid due to its surface tension. Figure B-1 illustrates the neck-in of the extruded flow. When the flow is extruded out of narrow slit, the flow is so thin that surface tension is the dominant force in determing its behavior. Maximum gap distance is also closely related to neck-ins. Figures B-2 and B-3 demonstrate the neck-in as a function of gap distance. It is obvious from these two plots that neck-in increases more rapidly as gap distance widens.

Studying the behavior of neck-in is very important in extrusion-spin coating. Initially uniform coating thickness depends on the amount of neck-in. Experiments to estimate the neck-in were conducted. The effect of neck-ins was observed using different parameters. Gap distance, flow rate, and viscosity of the photoresist were three parameters that influence neck-in.

Figure B-2 and Figure B-3 show the general trend of neck-in increase as the gap distance broadens and flow rate decreases. In addition, more viscous flow tends to neck-in less rapidly. Maximum gap distances are also indicated in both figures. The point at furthest right side among the same group indicate maximum gap distance. Drawdown ratios corresponding to maximum gap distances are obtained and specified
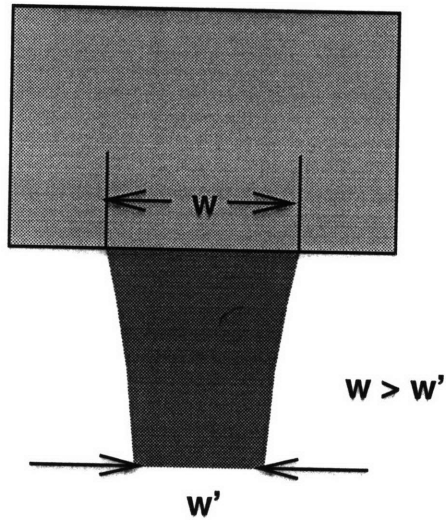
Figure B-1: Neck-in of extruded flow.

in both figures. Note that drawdown ratios of a specific resist stay in close range with one another. Drawdown ratio for each experiment must not exceed these values for a successful coating. However, as long as the drawdown ratio remains below the maximum values, it has been experimentally proved not to affect the coating result significantly.
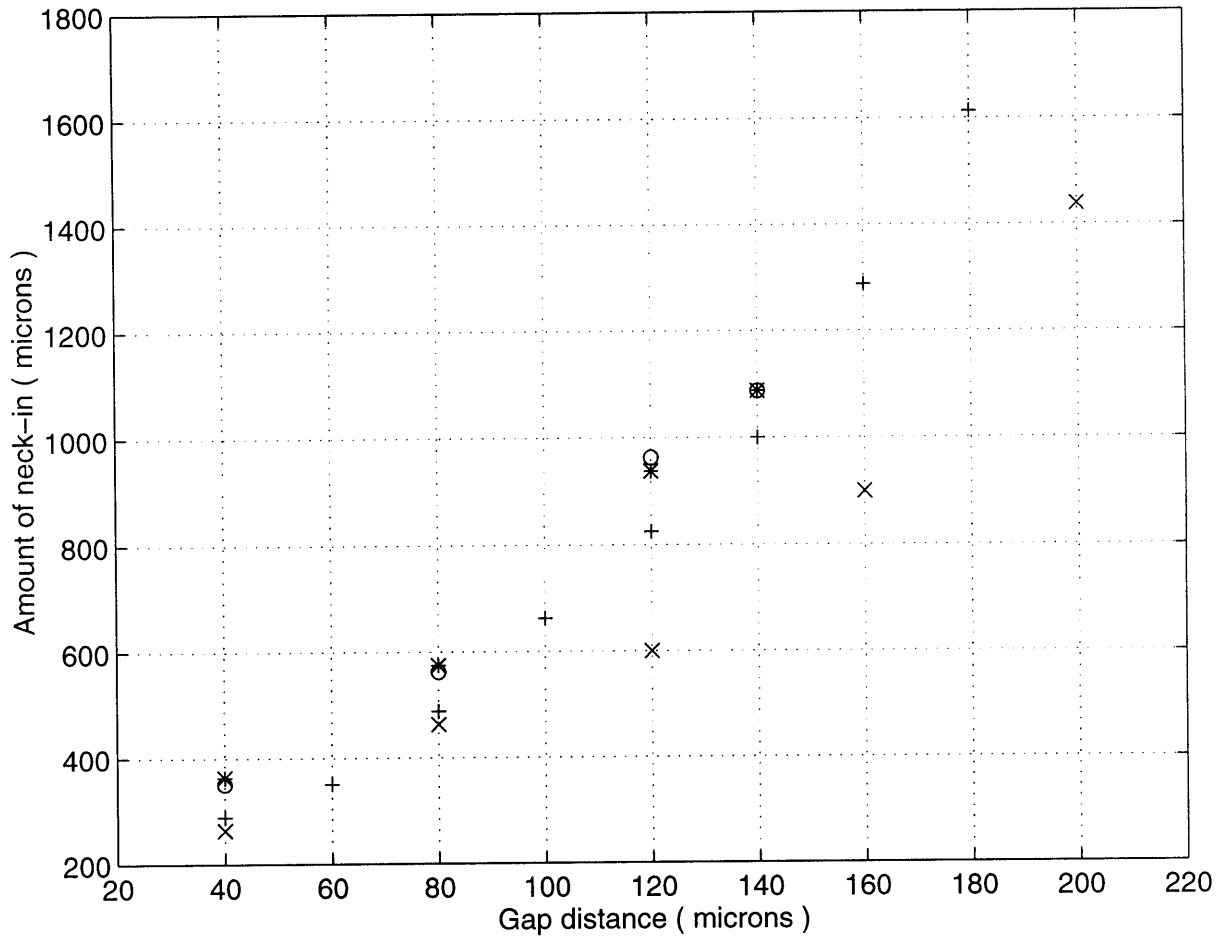
Figure B-2: Experimental data of neck-ins for AZ1512 photoresist. All points represent the amount of neck-ins with different gap distance and flow rate. (a) "+": 8 cm/sec, 0.04 ml/sec, DR=7.407, (b) "x": 8 cm/sec, 0.048 ml/sec, DR=6.944 (c) "*": 10cm/sec, 0.05 ml/sec, DR=5.688, (d) "o": 10 cm/sec, 0.06 ml/sec, DR=5.688.
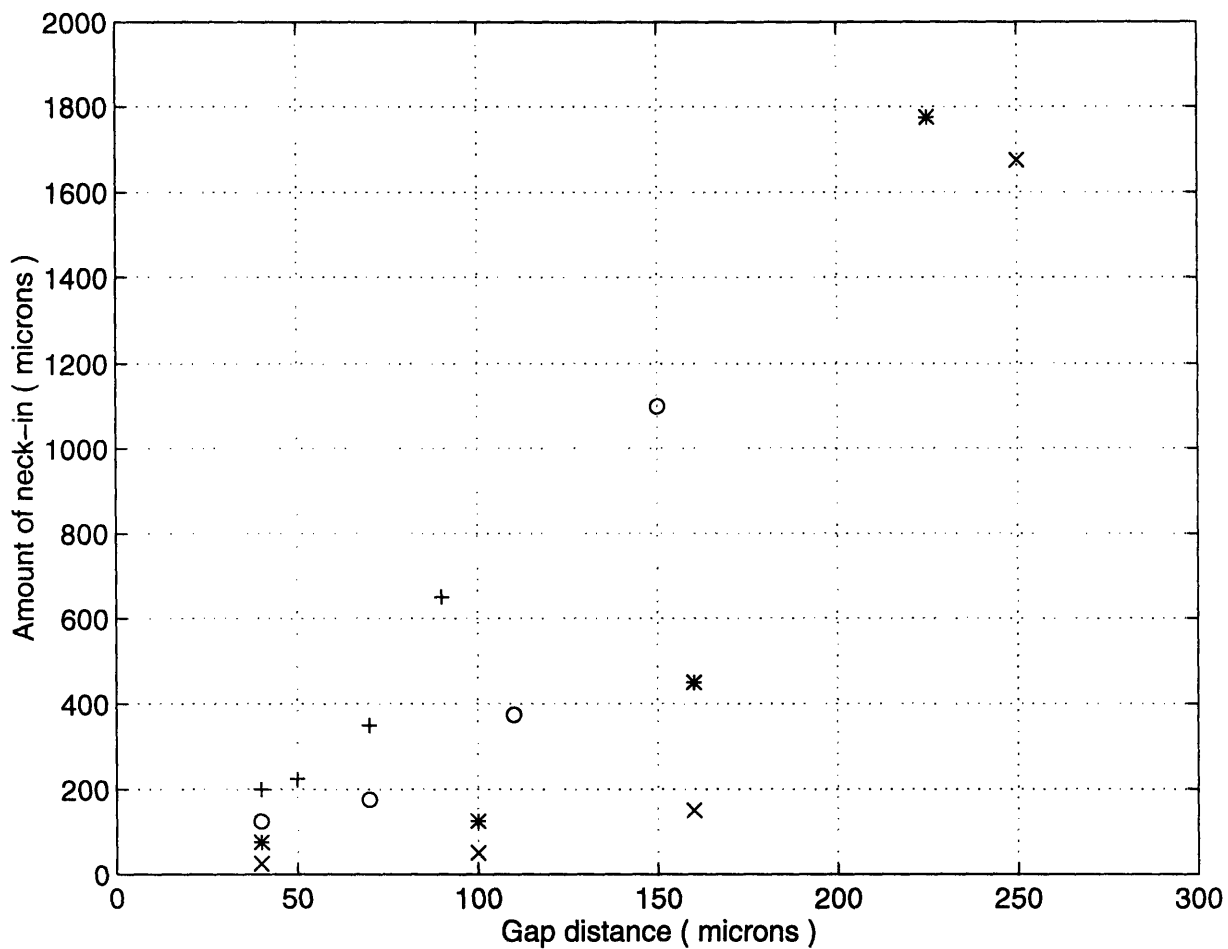
Figure B-3: Experimental data of neck-in's for Deep UV photoresist. All points represent the amount of neck-in's with different gap distance and flow rate. (a) "+": 0.0125 ml/sec, DR=11.236, (b) "o": 0.0156 ml/sec, DR=15 (c) "*": 0.0235 ml/sec, DR=15, (d) "x": 0.0313 ml/sec, DR=12.5.

Appendix C

Pump Calibration

The nominal lowest flow rate with the Millipore Gen2^{Plus} pump is 0.08 ml/sec. However, that does not include the uncompensated compliance of the supplying hose and resistance in extrusion die. The pump had to be calibrated to obtain the exact flow rate. Moreover, as 0.08 ml/sec was an unsatisfactory minimum flow rate for the application, a bleeding valve was designed and installed in addition to the existing valve. The bleeding valve consists of two components: an on-off valve and adjustment valve. On-off valve turns bleeding valve on and off. Adjustment valve controls the flow rate by regulating the number of turns. Figure C-1, indicating the pump calibration with AZ1512 photoresist, shows that the increase in flow rate is approximately linear until it reaches 0.065 ml/sec. Figure C-2 demostrates an interesting result. Flow rates with different total dispense volume tend to converge at low flow rates and diverge at high flow rates, which can be explained by error terms created by the pump. Errors occur in the low flow rate region. From the results, it is evident that the pump needs a certain amount of dispense before it reaches the steady state value. In this application, however, the pump does not reach a steady state flow rate before the dispense cycle ends, since the total dispense volume is low. This creates the aberrations from the expected value.

The desired flow rate for each photoresist can be estimated by correlating different points at the same number of turns of the adjustment valve.
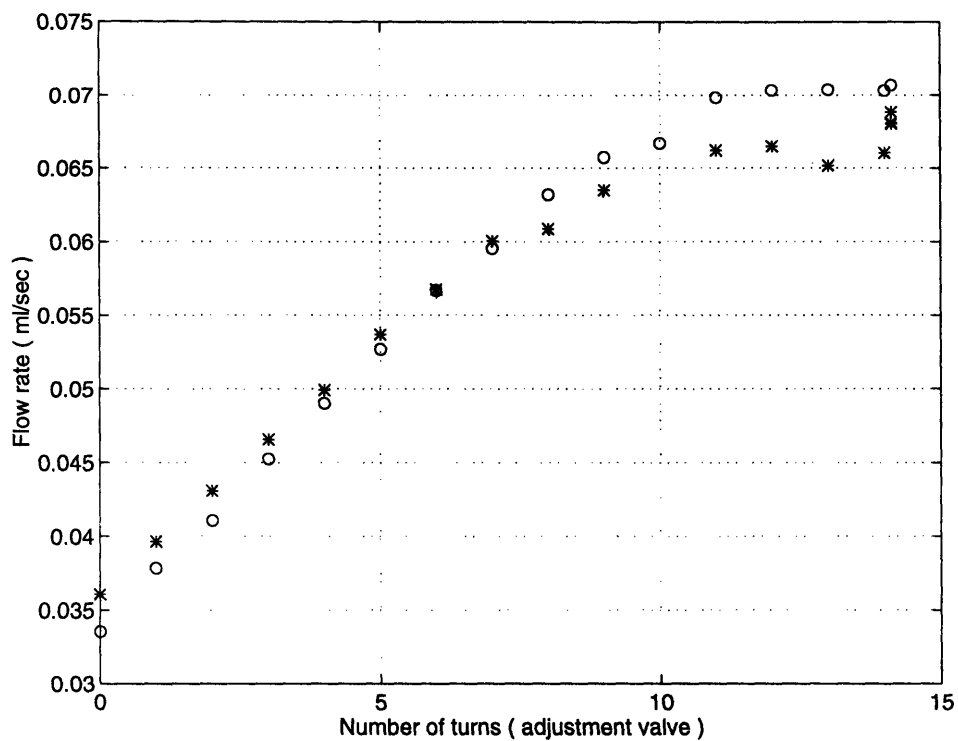
Figure C-1: Pump calibration with AZ1512 with 1 ml total dispense (∗) and 2 ml total dispense (o).
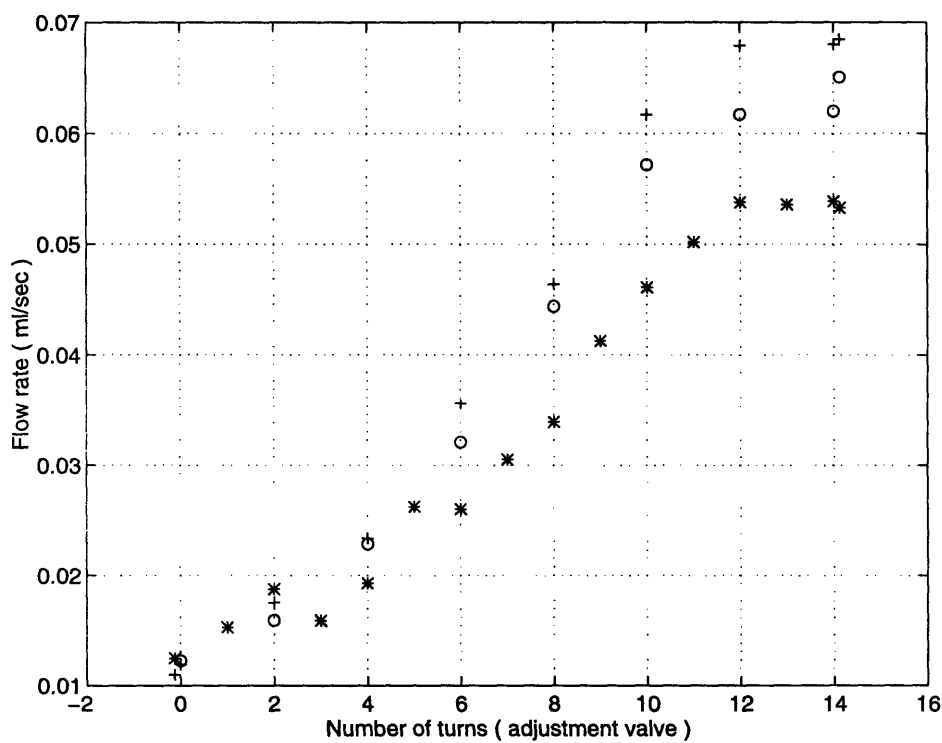

Figure C-2: Pump calibration with AZ Deep UV resist with 1 ml total dispense (∗), 2 ml total dispense (o), and 3 ml total dispense (+).

Bibliography

[1] Solid state technology, March 1991.

[2] A. E. Beguin. Method of coating strip material. U.S. Patent 2,681,294, 1954.

[3] N. E. Bixler. *Stability of a coating flow*. PhD thesis, University of Minnesota, 1982.

[4] R. Burley and B. S. Kennedy. An experimental study of air entrainment at a solid-liquid-gas interface. *Chem. Eng. Sci.*, 31, 1976.

[5] R. Burley and B. S. Kennedy. A study of dynamic wetting behavior of polyester tapes. *Br. polymer J.*, 8, 1976.

[6] R. Burley and B. S. Kennedy. *Wetting, spreading, and adhesion*, chapter 15. Academic Press, London, 1978.

[7] Edward J. Choinsky. Patch coating : Taking the spin out of thin. *Information Display*, November 1991.

[8] T. Daou and G. Webber. Semiconductor International, March 1995.

[9] W. J. Daughton and F. L. Givens. An investigation of the thickness variation of spin-on thin-films commonly associated with the semiconductor industry. *J. Electrochem. Soc.*, 129, 1982.

[10] B. M. Deryagin and S. M. Levi. Film coating theory. Focal Press, London, 1964.

[11] Alfred G. Emslie, Francis T. Booner, and Leslie G. Peck. Flow of a viscous liquid on a rotating disk. *Journal of Applied Physics*, 29, June 1957.

[12] Edgar B. Gutoff. *Modern Coating and Drying Technology*, chapter 4. VCH Publishers, Inc., 1992.

[13] Edgar. B. Gutoff. Simplified design of coating die internals. *Journal of imaging science and technology*, 37, 1993.

[14] Edgar B. Gutoff and Edward Cohen. *Coating and Drying Defects*, chapter 7. John Wiley and Sons, New York, 1995.

[15] P. Joos and E. Rillaerts. The dynamic contact angle. *Chem. Eng. Sci.*, 35, 1980.

[16] K. Y. Lee, L. D. Liu, and T. J. Liu. Minimum wet thickness in extrusion slot coating. *Chem. Eng. Sci.*, 47, 1992.

[17] D. Meyerhofer. Characteristics of resist films produced by spinning. *J. Appl. Phys.*, 49, 1978.

[18] Wayne M. Moreau. *Semiconductor Lithography: Principles, Practices and Materials*, chapter 1. Plenum Press, New York, 1988.

[19] W. Mues, J. Hens, and L. Boiy. Observation of a dynamic wetting process using laser-doppler velocimetry. *AIChE*, 35, 1989.

[20] R. T. Perry. *Fluid Mechanics of Entrainment Through Liquid-Liquid and Liquid-Solid Junctions*. PhD thesis, University of Michigan, 1966.

[21] Kenneth J. Ruschak. Limiting flow in a pre-metered coating device. *Chem. Eng. Sci*, 31, 1976.

[22] Luigi Sartor. *Slot Coating: Fluid Mechanics and Die Design*. PhD thesis, University of Minnesota, 1990.

[23] Peter C. Sukanek. Dependence of film thickness on speed in spin coating. *J. Electrochem. Soc.*, 138, June 1991.

[24] John A. Tallmadge, Charles B. Weinberger, and Helen L. Faust. Bead coating instability : A comparison of speed limit data with theory. *AIChE*, 25, 1979.

[25] S. Wolf and R. N. Tauber. *Silicon Processing for the VLSI Era: Volume 1 - Process Technology*, chapter 12. Lattice Press: Sunset Beach, CA, 1986.

[26] A. Zimmerman and E. Fahrni. Coating device. U.S. Patent 4,109,611, April 1978.